

Article

A Mass Spectrometry-Based Approach for Characterization of Red, Blue, and Purple Natural Dyes

Katarzyna Lech ^{1,*}  and Emilia Fornal ² ¹ Faculty of Chemistry, Warsaw University of Technology, Noakowskiego 3, 00-664 Warsaw, Poland² Department of Pathophysiology, Medical University of Lublin, Jaczewskiego 8b, 20-090 Lublin, Poland; emilia.fornal@umlub.pl

* Correspondence: klech@ch.pw.edu.pl

Academic Editor: Pascal Gerbaux

Received: 21 June 2020; Accepted: 13 July 2020; Published: 15 July 2020



Abstract: Effective analytical approaches for the identification of natural dyes in historical textiles are mainly based on high-performance liquid chromatography coupled with spectrophotometric detection and tandem mass spectrometric detection with electrospray ionization (HPLC-UV-Vis-ESI MS/MS). Due to the wide variety of dyes, the developed method should include an adequate number of reference color compounds, but not all of them are commercially available. Thus, the present study was focused on extending of the universal analytical HPLC-UV-Vis-ESI MS/MS approach to commercially unavailable markers of red, purple, and blue dyes. In the present study, HPLC-UV-Vis-ESI MS/MS was used to characterize the colorants in ten natural dyes (American cochineal, brazilwood, indigo, kermes, lac dye, logwood, madder, orchil, Polish cochineal, and sandalwood) and, hence, to extend the analytical method for the identification of natural dyes used in historical objects to new compounds. Dye markers were identified mostly on the basis of triple quadrupole MS/MS spectra. In consequence, the HPLC-UV-Vis-ESI MS/MS method with dynamic multiple reaction monitoring (dMRM) was extended to the next 49 commercially unavailable colorants (anthraquinones and flavonoids) in negative ion mode and to 11 (indigoids and orceins) in positive ion mode. These include protosappanin B, protosappanin E, erythrolaccin, deoxyerythrolaccin, nordamnacanthal, lucidin, santalin A, santalin B, santarubin A, and many others. Moreover, high-resolution QToF MS data led to the establishment of the complex fragmentation pathways of α -, β -, and γ - aminoorceins, hydroxyorceins, and aminoorceinimines extracted from wool dyed with *Rocella tinctoria* DC. The developed approach has been tested in the identification of natural dyes used in 223 red, purple, and blue fibers from 15th- to 17th-century silk textiles. These European and Near Eastern textiles have been used in vestments from the collections of twenty Krakow churches.

Keywords: natural dyes; orchil; sandalwood; brazilwood; tandem mass spectrometry; textile

1. Introduction

High-performance liquid chromatography (HPLC) is the most common technique used for the separation of colorants present in natural dyes and historical textiles [1–3]. Since the amount of available research material is usually limited, it is extremely important to use a sensitive detector that is both selective and versatile for a variety of coloring compounds. Thus, the best results are acquired using both spectrophotometric (UV-Vis) and mass spectrometric (MS) detection together [4–13]; however, they are used individually as well [14–22].

The best separations to date have been achieved using reversed phase columns, mostly C18. However, since colorants have extended systems of conjugated double bonds, it seems reasonable to

use columns with phenyl-type stationary phases capable of exploiting pi–pi interactions to achieve separation. The correct identification of a dye requires, at first, the true positive identification of analytes, which has to be based on the comparison of not only their retention times but also their other physicochemical properties (such as m/z values and characteristic absorption) with those of reference compounds determined under identical experimental conditions. Therefore, it is important to prepare a wide/extensive database of markers covering the largest possible number of dyes.

Unfortunately, some of the colorants are commercially unavailable, and thus, their identification can be troublesome. Therefore, a tandem mass spectrometer (MS/MS) as an HPLC detector turns out to be extremely useful. Since the fragmentation pathways of colorants within classes are rather similar, some ions may have diagnostic functions [12,23–26]. They can provide structural information about eluted compounds [27–29], providing a basis for their identification. Moreover, a tandem mass spectrometer with a triple quadrupole offers multiple reaction monitoring (MRM), which is particularly useful for the specific analysis of target compounds in complex mixtures.

Most HPLC methods published to date have been dedicated to identifying specific groups of colorants, such as anthraquinones from madder and scale insects [7–11,14,17–22,30,31] or indigoids [5,7–9,11–16,20,21,32], whereas only one was about orchil colorants [33–35]. However, it appears that there are no reports devoted to sandalwood colorants. Additionally, not all brazilwood markers have been identified yet, despite recent successes in this field [36]. Furthermore, to the best of our knowledge, there is no publication on a universal analytical approach discussing dozens of colorants, as opposed to being limited to just selected and the most popular compounds or their groups.

The present study was focused on the development of a comprehensive analytical approach for the identification of natural dyes in historical objects, antiques, and works of art. To do so, research was carried out using high-performance liquid chromatography coupled with spectrophotometric detection and tandem mass spectrometric detection with electrospray ionization (HPLC-UV-Vis-ESI MS/MS) and quadrupole time-of-flight mass spectrometry (QToF MS), which resulted in the determination of commercially unavailable markers present in ten red, purple, and blue dyes (American cochineal, brazilwood, indigo, kermes, lac dye, logwood, madder, orchil, sandalwood, and Polish cochineal). It led, among that of others, to the identification of α -, β -, and γ -aminoorceins, hydroxyorceins, and aminoorceinimines in wool dyed with *Rocella tinctoria* DC and, thanks to high-resolution data, to the specification of their complex fragmentation pathways. As a consequence, the new markers were introduced to the HPLC-UV-Vis-ESI MS/MS developed method. This became a base for creating an analytical approach that combines an extraction protocol and detection parameters (UV-Vis and MS) depending on sample color and, consequently, on pending analytes. This approach was subsequently applied to analyze 223 thread samples from silk textiles dated from the 15th to 17th century and used in vestments from the collections of twenty Krakow churches. The obtained results—together with already-published data on yellow, brown, and green threads [37,38]—have completed the picture of natural dyes used in the most valuable 15th- to 17th-century textiles of European and Near Eastern origin.

2. Results and Discussion

The previously developed HPLC-UV-Vis-MS/MS method (incorporating commercially available standards and markers of yellow, orange, and brown dyes) [37] was extended to colorants present in another ten dyes (American cochineal, brazilwood, indigo, kermes, lac dye, logwood, madder, orchil, sandalwood, and Polish cochineal). The compounds were identified according to the MS/MS spectra acquired for various collision energies (CEs). The most intense precursor and product ion pairs (transitions) of the identified dye markers were used to develop the final method in dynamic multiple reaction monitoring (dMRM) mode, which provides superior sensitivity and selectivity for targeted compounds in complex samples. In a dMRM experiment, analytes are only monitored while they are being eluted from the LC (during the retention window), so the MS duty cycle is not wasted by monitoring them when they are not expected, which maximizes the detection capability of the MS.

The first quadrupole is set to pass a desired precursor ion, the second quadrupole is used as a collision cell to fragment that precursor ion, and the third quadrupole is set to monitor a specific fragment ion. The new colorants and their MS transitions are shown in detail in Table 1. Consequently, the method was applied to investigate dyes used in 15th- to 17th-century textiles.

Table 1. High-performance liquid chromatography coupled with spectrophotometric detection and tandem mass spectrometric detection with electrospray ionization (HPLC-UV-Vis-ESI MS/MS) characterization of color compounds.

No	Compound Name	t_R , min	$[M - H]^-$, m/z	Frag., V	Product Ions, m/z (CE, V)	λ_{max} , nm
1	hematein *	4.0	299	130	281 (8), 253 (15), 174 (20), 125 (20)	284, 383
2	hematoxylin *	5.2	301	150	283 (17), 179 (15), 137 (21), 123 (29)	279, 397
3	brazilein	5.5	283	130	265 (25), 174 (25), 145 (25), 109 (25)	
4	hc1	5.8	319	90	259 (15), 247 (15), 241 (15), 227 (15)	
5	protosappanin B	6.6	303	130	231 (15)	
6	brazilin	7.1	285	110	163 (25), 135 (30), 121 (30)	
7	hc3 (hematoxylin dimer)	7.2	603	150	301 (20), 179 (20)	
8	laccic acid E	7.9	494	90	450 (10), 406 (20)	228, 288, 492
9	deoxyerythrolaccin di-O-hexoside (pp2)	8.0	593	170	431 (25), 269 (35)	
10	hc2	8.2	317	90	195 (15), 152 (15), 125 (30)	
11	caes1 (brazilin-like)	8.4	285	130	257 (15), 243 (25), 214 (25)	
12	kermesic acid di-C-hexoside (pp3)	8.5	653	170	609 (20), 357 (30), 327 (30)	
14	caesD	9.3	303	130	245 (10), 227 (10), 217 (25)	
15	hc4 (dimer)	9.4	581	150	281 (25)	
16	laccic acid C	9.5	538	90	494 (10), 450 (20)	228, 288, 492
17	flavokermesic acid O-hexoside (pp6/pp1)	10.3	475	170	431 (15), 269 (25)	285, 339, 399
18	flavokermesic acid 2-C-glucoside (dclI)	10.5	475	170	431 (13), 341 (22), 311 (22), 282 (41)	287, 435
19	carminic acid *	11.2	491	170	447 (14), 357 (22), 327 (22), 299 (34)	276, 310, 496
20	kermesic acid O-hexoside (pp7/ppII)	11.8	491	170	447 (15), 285 (25)	276, 466
21	uroolithin C	13.9	243	130	215 (25), 199 (25), 187 (25)	
22	dc3	14.5	535	170	473 (20), 445 (30), 415 (25)	
23	flavokermesic acid 6-O-glucoside (dcOfka)	14.8	475	170	431 (20), 268 (35), 240 (45)	280, 342, 431
24	carminic acid derivative	15.1	519	170	475 (15), 357 (25), 327 (25), 298 (40)	
25	dc4	15.5	519	170	397 (30), 385 (25), 327 (35)	
26	protosappanin E	16.2	585	90	283 (15)	
27	kermesic acid O-hexoside (pp9)	16.3	491	170	447 (18), 284 (25)	
28	caes2 (brazilin-like)	16.4	285	130	161 (15), 134 (25)	
29	deoxyerythrolaccin O-hexoside (pp10)	16.5	431	170	269 (25)	
30	kermesic acid 7-C-glucofuranoside (dclV)	16.8	491	170	447 (15), 357 (25), 327 (35), 299 (40)	277, 314, 493
34	xantholaccic acid B	17.4	479	90	435 (10), 391 (25)	
35	lucidin O-primeveroside	17.9	563	130	269 (10), 251 (45)	246, 266, 342, 407
36	kermesic acid 7-C-glucofuranoside (dcVII)	18.4	491	170	447 (15), 357 (25), 327 (30), 299 (35)	277, 312, 492
38	ruberthric acid	18.5	533	130	239 (18)	228, 258, 334, 416
39	laccic acid B	19.2	495	90	451 (10), 407 (20), 389 (35)	230, 288, 492
40	xantholaccic acid A	19.4	520	90	476 (10), 432 (25)	230, 288, 492
41	deoxyerythrolaccin O-hexoside (pp12)	21.5	431	170	268 (30)	
42	anthraflavic acid *	21.6	239	130	211 (26), 210 (30), 195 (22), 182 (42)	240, 273, 299, 346
43	laccic acid A	21.6	536	90	492 (10), 448 (18), 430 (30), 358 (45)	228, 288, 492
48	rubidiin O-primeveroside	22.6	547	130	253 (20)	
50	anthragallol	23.6	255	130	227 (25), 153 (35), 125 (35)	
51	flavokermesic acid	23.6	313	90	269 (10)	284, 342, 431
52	kermesic acid *	24.2	329	90	285 (10)	274, 308, 492
53	kermesic acid O-hexoside derivative (1) (pp14)	25.5	589	170	545 (20), 357 (25), 327 (25)	
54	lucidin	25.7	299	130	251 (15), 223 (30), 195 (35)	
55	alizarin *	26.4	239	170	211 (26), 210 (30)	248, 274, 324, 429
57	deoxyerythrolaccin	27.2	269	130	241 (25), 225 (25)	
59	anthrarufin *	27.4	239	170	211 (26), 182 (45)	225, 252, 285, 417
60	kermesic acid O-hexoside derivative (2) (pp15)	27.4	617	170	545 (20), 357 (25), 327 (25)	
61	xanthopurpurin	27.5	239	130	211 (25), 195 (25)	
62	santalalin A	27.6	581	130	566 (25), 551 (32), 523 (40)	
63	erythrolaccin	27.9	285	130	257 (25), 241 (25)	
64	purpurin *	28.3	255	130	227 (22), 171 (30), 129 (38), 101 (45)	255, 290, 482
66	rubidiin *	29.0	253	110	225 (25), 209 (22), 195 (55)	245, 278, 330, 411
68	santalalin B	29.8	595	130	580 (25), 565 (35)	
69	chryszarin *	29.8	239	170	211 (26)	223, 252, 283, 428
70	quinizarin *	30.1	239	210	211 (18)	224, 248, 278, 324, 479
71	ps1 (santalalin-like)	30.2	503	130	488 (20), 473 (25), 445 (25)	
72	nordamcanthal	30.5	267	90	239 (14), 211 (25), 195 (34)	259, 294, 418
73	chrysofhanol *	30.8	253	170	225 (26)	225, 256, 277, 287, 429
74	santarubin A	30.9	609	130	594 (25), 579 (25), 551 (40)	
75	atranorin *	31.0	373	90	177 (10), 163 (14), 133 (22)	
76	rt1 (alizarin-lucidin O-dimer)	32.1	491	150	251 (25), 239 (35)	
13	isatin *	8.8	148	90	130 (15), 102 (25), 92 (20), 77 (25), 65 (30)	296, 413
31	indigoid compound A	17.2	262	90	235 (30), 219 (30), 190 (40), 120 (30)	
32	β/γ -aminoocein	17.2	485	140	470 (45), 415 (40), 362 (42)	
33	β/γ -aminooceinimine	17.3	484	140	469 (50), 468 (42), 361 (50)	
37	indigoid compound B	18.4	262	90	234 (20), 219 (20), 31 (30)	
44	β/γ -hydroxyorcein	21.7	486	140	471 (45), 469 (40), 416 (40)	
45	α -aminooceinimine	21.9	362	140	347 (38), 331 (45), 278 (40)	
46	β/γ -aminooceinimine	22.0	484	140	469 (45), 424 (55), 362 (42)	
47	β/γ -aminoocein	22.3	485	140	470 (42), 415 (40), 362 (42)	
49	α -aminoocein	22.7	363	140	348 (28), 347 (32), 303 (40), 240 (36)	
56	β/γ -hydroxyorcein	26.6	486	140	471 (45), 416 (42)	
58	α -hydroxyorcein	27.3	364	140	349 (30), 344 (25), 294 (25), 279 (40)	
65	indigotin *	28.7	263	90	235 (23), 219 (19), 206 (39), 132 (35), 77 (50)	291, 620 #
67	indirubin *	29.2	263	170	235 (19), 219 (23), 190 (43)	257, 550 #

* Data determined for standard solutions and presented in [37], # absorption maxima determined for DMSO solutions.

2.1. Dyes

Colorants extracted from indigo as well as from wool fibers dyed with nine other dyes were identified using an ESI MS/MS detector preceded by HPLC with a phenyl column. Full scan analysis and the subsequent MS/MS fragmentations of the predominant quasi-molecular ions were used to obtain information about the molecular weights of the colorants and for the structural evaluation of the sugar moieties, aglycones, and unglycosylated compounds.

2.1.1. Indigo

Chromatograms acquired for a DMSO extract of indigo showed two main peaks that corresponded to indigotin (65) ($[M + H]^+$ at m/z 263) and indirubin (67) ($[M + H]^+$ at m/z 263). They were observed with a spectrophotometer at 280, 550, and 600 nm and with an MS detector in positive ion mode. In addition, two small peaks were found at t_R 17.2 and 18.4 min (Figure 1a). The MS investigation of these two compounds suggested that they might be isomers. Firstly, the even m/z values of both their $[M + H]^+$ ions were 262, which indicated an odd number of nitrogen atoms in their molecules. Secondly, their MS/MS spectra were very similar to each other although not identical (Supplementary Materials, Figure S1). Apart from the ions at m/z 245, 235, 219, and 190 present in both mass spectra, the first compound (t_R 17.2 min) showed an intense signal at m/z 120, whereas the second one (t_R 18.4 min) showed such at m/z 131. These MS/MS spectra almost completely coincided with those acquired for indigotin and indirubin, especially for m/z values above 150, indicating similarities between their structures too. Looking at the data taken together, the chemical formula of both compounds was defined as $C_{16}H_{11}N_3O$; however, their molecular structures could not be determined. Nevertheless, it seemed that these compounds (called indigoid compound A (31) and B (37)) would not be crucial for identifying indigo in historical objects.

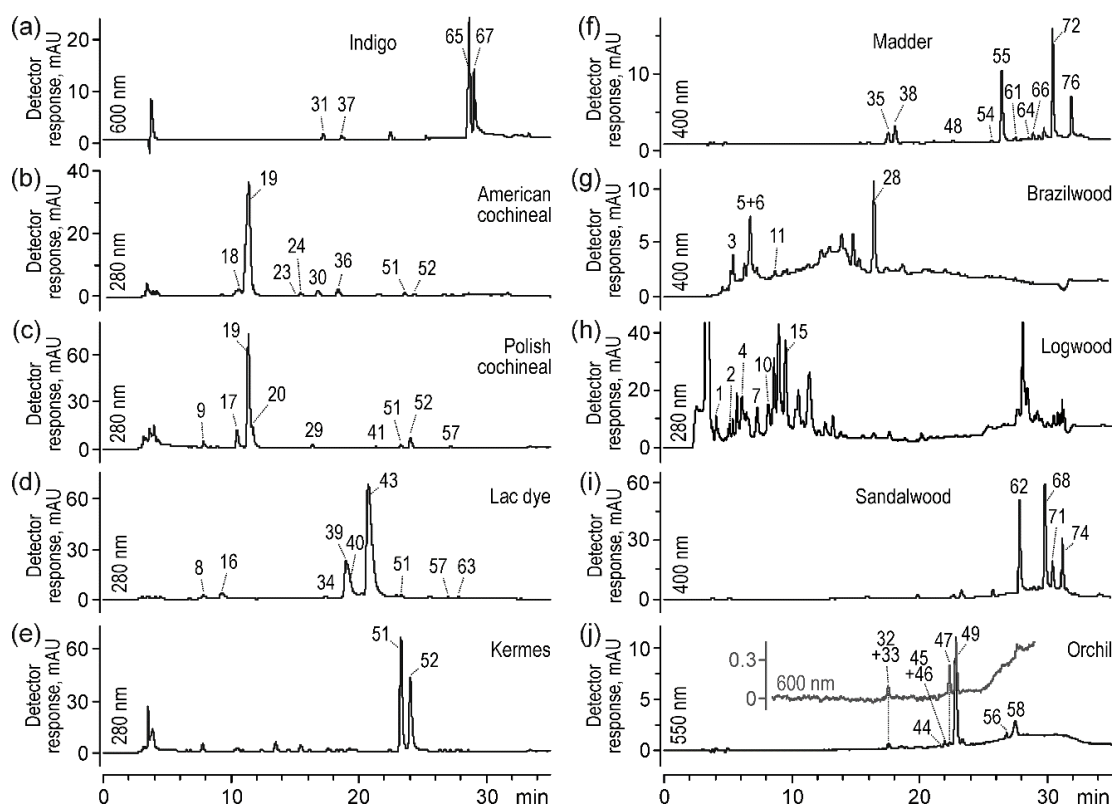


Figure 1. Chromatogram of Polynesian indigo (a), American cochineal (b), Polish cochineal (c), lac dye (d), kermes (e), madder (f), brazilwood (g), logwood (h), sandalwood (i), and orchil (j) extracts acquired by UV-Vis detector; peak numbers are decoded in Table 1.

2.1.2. Scale Insect Dyes

Colorants present in American and Polish cochineals were the subject of earlier detailed studies [24,25]. On this basis, apart from carminic and kermesic acids (52), flavokermesic acid (51), dcII (18), dcIV (30), dcVII (36), dcOfka (23), dc3 (22), and dc4 (25) (Figure 1b) as well as pp6 (17), pp7 (20), and deoxyerythrolaccin (57) (Figure 1c) were included in the presented method, as they were previously recommended as American and Polish cochineal markers, respectively.

Chromatographic and spectrometric data acquired for the lac dye extract proved the presence of several laccacic and xantholaccaic acids [39] (Figure 1d). Since they are animal-origin oxidized derivatives of kermesic and flavokermesic acids substituted at the C-7 position by a large functional group (Supplementary Materials, Figure S2)—that is, by *N*-acetyltyramine (in laccaic acid A and xantholaccaic acid A), tyrosal (laccaic acid B and xantholaccaic acid B), tyrosine (laccaic acid C), or tyramine (laccaic acid E)—their $[M - H]^-$ ions showed almost identical fragmentation pathways. The two most intense signals in each MS/MS spectrum (Supplementary Materials, Figure S3) corresponded to the loss of one or two CO_2 molecules from carboxyl groups, whereas the next one was a result of the further loss of a H_2O molecule.

Apart from laccaic and xantholaccaic acids, the lac dye extract also contained kermesic acid (52) ($[M - H]^-$ at m/z 329) and flavokermesic acid (51) ($[M - H]^-$ at m/z 313), as well as their decarboxylated derivatives, erythrolaccin (63) ($[M - H]^-$ at m/z 285) and deoxyerythrolaccin (57) ($[M - H]^-$ at m/z 269). Their fragmentation pathways were also similar to each other. The signals at m/z 257, 241, 229, and 213 for erythrolaccin (Figure 2a) and at m/z 241, 225, 213, and 197 for deoxyerythrolaccin (Figure 2b) corresponded to the $[M - H - CO]^-$, $[M - H - CO_2]^-$, $[M - H - 2CO]^-$, and $[M - H - CO_2 - CO]^-$ ions, respectively.

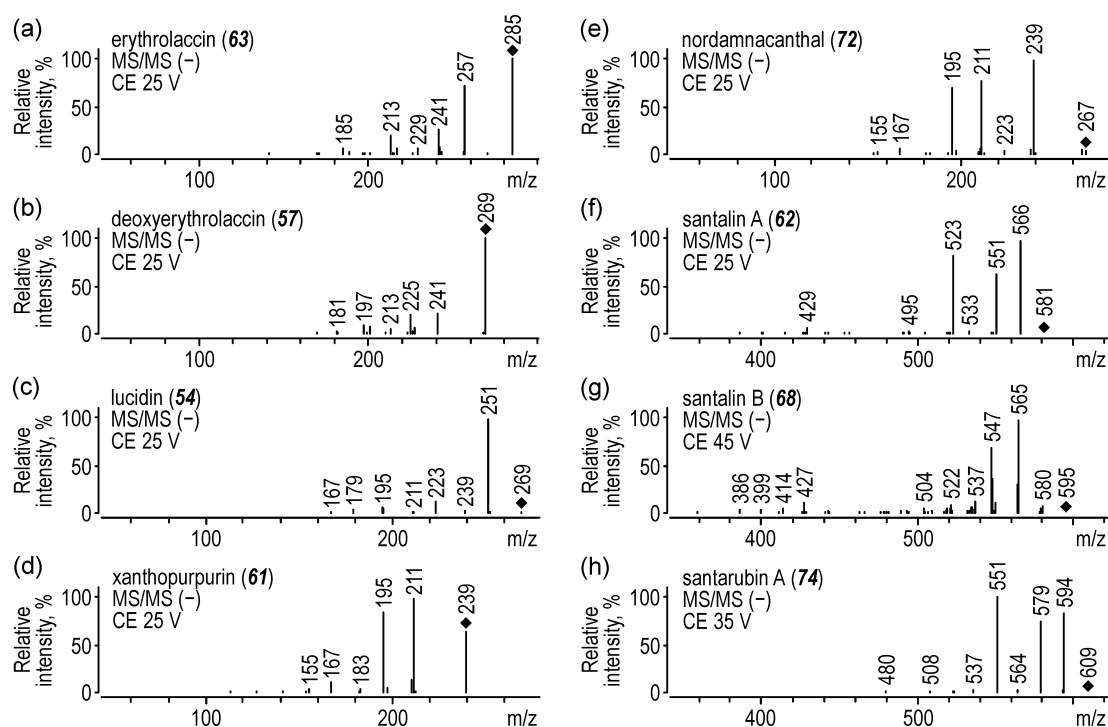


Figure 2. MS/MS spectra of (a) erythrolaccin, (b) deoxyerythrolaccin, (c) lucidin, (d) xanthopurpurin, (e) nordamnacanthal, (f) santalin A, (g) santalin B, and (h) santarubin A acquired in negative ion mode.

Chromatograms of the kermes extract (Figure 1e) showed two main peaks of kermesic acid (52) and flavokermesic acid (51) as well as traces of deoxyerythrolaccin (57). Next, two small peaks eluted at 10.5 and 16.3 min were identified to be pp6 (17) (flavokermesic acid *O*-hexoside, m/z 475–431, 269) and pp9 (27) (kermesic acid *O*-hexoside, m/z 491–447, 284), respectively. Their MS/MS spectra showed

the same fragmentation pattern, according to which the first signals corresponded to the $[M-H-CO_2]^-$ ions, and the next ones were formed by the subsequent loss of hexose moieties ($[M-H-CO_2-Hex]^-$ or $[M-H-CO_2-Hex]^-$).

2.1.3. Madder

Chromatograms of the madder extract acquired by the spectrophotometric detector showed several peaks. The most intense peak belonged to alizarin (55), but purpurin (64) and rubiadin (66) were also found (Figure 1f). These colorants were identified by comparison with their standards, while others required the analysis of MS/MS spectra.

A compound eluted just before alizarin and observed in the chromatograms acquired at 280 and 400 nm was identified to be lucidin (54). MS/MS spectra of its $[M - H]^-$ ion at m/z 269 (Figure 2c) showed three intense signals at m/z 251, 223, and 295 corresponding to the loss of H_2O from a terminal aliphatic hydroxyl group and to the further elimination of one or two CO molecules, respectively. Compounds eluted at t_R 27.5 and 30.5 min were identified to be xanthopurpurin (61) ($[M - H]^-$ at m/z 239, Figure 2d) and nordamnacanthal (72) ($[M - H]^-$ at m/z 267, Figure 2e), respectively. They differ from each other only by the presence of an aldehyde group at the C-2 position of nordamnacanthal that fragmented in the first place, giving the $[M-H-CO]^-$ ion at m/z 239. Apart from that, all the other signals in both spectra were the same; the ions at m/z 211, 195, and 167 were formed by the further loss of CO, CO_2 , or both of these molecules together, respectively. The MS/MS spectra of xanthopurpurin and nordamnacanthal were identical to those ones found in the literature [40,41]. Similar congruence was found for the absorbance spectra of other identified compounds.

Another peak was observed at 32.1 min in the chromatograms acquired with spectrophotometric detection at visible range. This compound (coded as rt1) has not been reported to date. Simple MS/MS spectra of its $[M - H]^-$ ion at m/z 491 included only two significant signals (Supplementary Materials, Figure S4), the first one at m/z 239 and the second one at m/z 251. It led to the assumption that the colorant was an anthraquinone dimer, probably composed of one alizarin molecule and one lucidin molecule (76).

Apart from the anthraquinones described above, some of their glycosidic derivatives were found, that is, lucidin *O*-primeveroside (35) ($[M - H]^-$ at m/z 563), ruberthyric acid (38) ($[M - H]^-$ at m/z 533), and rubiadin *O*-primeveroside (48) ($[M - H]^-$ at m/z 547). They were identified mainly thanks to the characteristic loss of 294 Da corresponding to the primeverosyl moiety, and by the comparison of their further fragments with those observed for lucidin (54), alizarin (55), and rubiadin (66) (Supplementary Materials, Figure S5).

2.1.4. Brazilwood

According to the literature, brazilwood contained mainly brazilin (6) and brazilein (3). Peaks of these two compounds were found at t_R 7.1 and 5.5 min, respectively, in the chromatogram of the brazilwood extract (Figure 1g). Their identification was based on MS/MS spectra.

The fragmentation of brazilin-type neoflavonoids has been discussed in only one publication to date [42], but the considerations have been devoted to one particular fusion, and they have not included the complete pathway, especially for brazilin. Nevertheless, the presented data were helpful in the identification of both neoflavonoids.

The fragmentation of brazilin and brazilein proceeded according to two mechanisms, that is, the loss of small neutral molecules or the cleavage of internal rings (their MS/MS spectra and the proposed directions of their fragmentation are shown in Figure 3a,b). The MS/MS spectra of brazilein (3) (m/z 283 $[M - H]^-$) showed signals at m/z 265 $[M-H-H_2O]^-$, 255 $[M-H-CO]^-$, 237 $[M-H-H_2O-CO]^-$, and 196 $[M-H-H_2O-CO-C_2HO]^-$. Moreover, C-ring fission led to the formation of intense ions at m/z 174 $[^{1,4}BD - H]^-$, 173 $[^{1,4}BD - H]^-$, 161 $[^{2,4}BD - H]^-$, 145 $[^{1,4}BD-H-CO]^-$, and 109 $[^{1,4}A - H]^-$. In the case of brazilin (6) (m/z 285 $[M - H]^-$), fragmentation occurred mostly via D-ring cleavage, mainly giving the ion at m/z 163 $[^{5,6}A - H]^-$, as well as the lower signals at m/z 135 $[^{5,6}A-H-CO]^-$,

121 [$^{5,6}\text{B} - \text{H}]^-$ (or [$^{2,4}\text{A} - \text{H}]^-$), and 109 [$^{5,7}\text{B} - \text{H}]^-$. The intensities of other signals corresponding to the losses of small molecules (m/z 267 [$\text{M} - \text{H} - \text{H}_2\text{O}]^-$, 239 [$\text{M} - \text{H} - \text{CO}_2$] $^-$, 227 [$\text{M} - \text{H} - \text{H}_2\text{O} - \text{CO}]^-$, and 211 [$\text{M} - \text{H} - \text{C}_3\text{H}_6\text{O}_2$] $^-$) were rather low. On this basis, it can be assumed that compounds classified as brazilin-type homoisoflavonoids with a fused five-membered D-ring [43] decompose mostly via this D-ring, whereas their oxidized forms, with an extra unsaturated bond in a D-ring that prevent their fission, fragment via a heterocyclic C-ring.

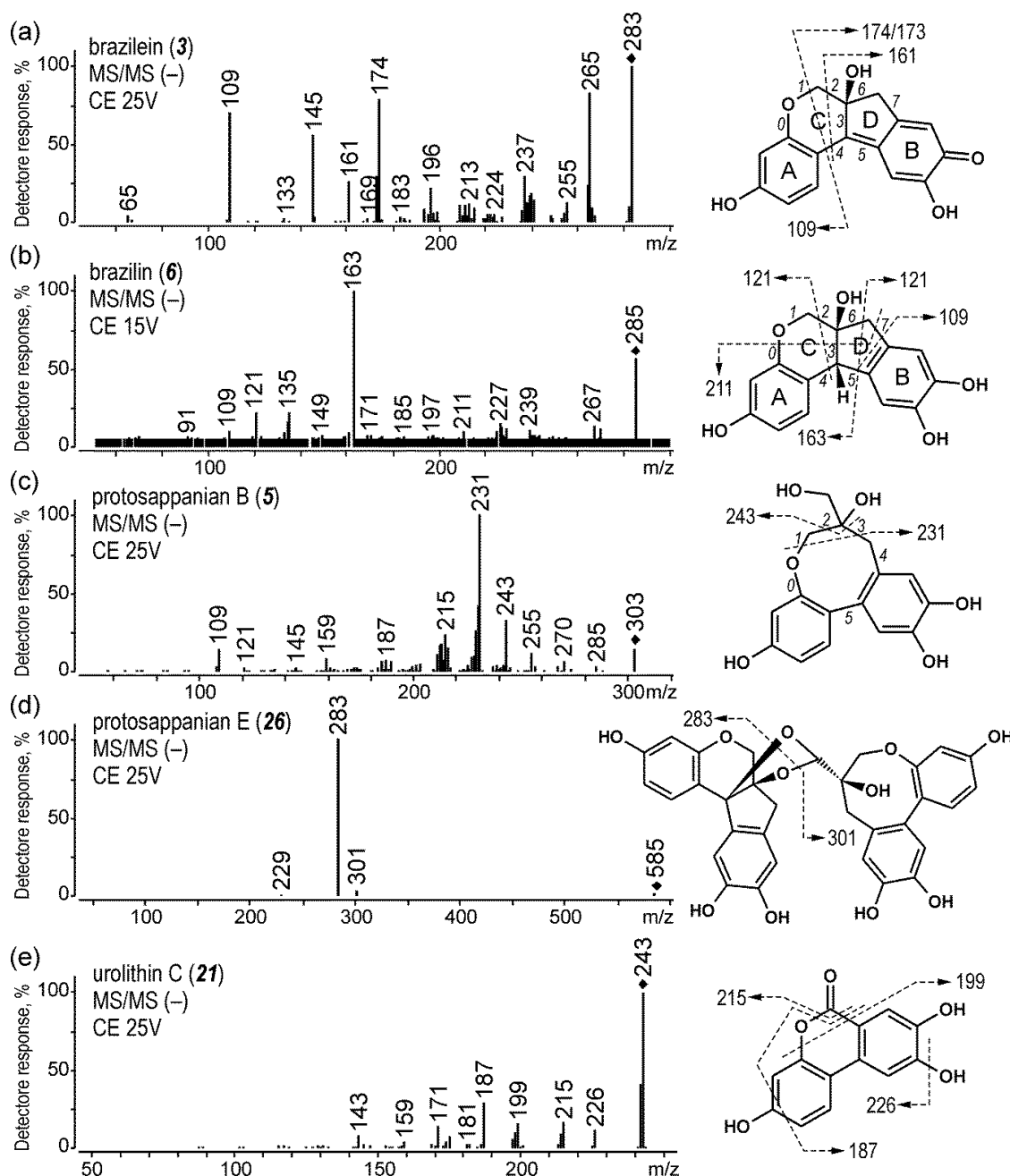


Figure 3. MS/MS spectra acquired in negative ion mode, and proposed fragmentation directions for (a) brazilin, (b) brazilin, (c) protosappanin B, (d) protosappanin E, and (e) urolithin C extracted from wool dyed with brazilwood.

The next two compounds eluted at 6.6 and 16.2 min were recognized to be protosappanin B (5) (m/z 303 [$\text{M} - \text{H}]^-$) and protosappanin E (26) (m/z 585 [$\text{M} - \text{H}]^-$), respectively. The MS/MS spectra of the former one (Figure 3c) showed two main ions at m/z 243 [$\text{M} - \text{H} - \text{C}_2\text{H}_4\text{O}_2$] $^-$ and 231 [$\text{M} - \text{H} - \text{C}_3\text{H}_4\text{O}_2$] $^-$

formed by inner ring cleavage. The fragmentation of prottosappanin E, which is a combination of brazilin and protosappanin B molecules, was even simpler, since it resulted in only one signal at m/z 283 (Figure 3d). Probably, it was formed by the decomposition of bonds between both moieties.

Moreover, two brazilin-like compounds (**11**, **28**) were also found (t_R 8.4 and 16.4 min, both $[M - H]^-$ at m/z 285). Their MS/MS spectra (Supplementary Materials, Figure S6) were like those of brazilin, but their structures remain unknown. Probably, they were brazilin isomers, or they belonged to homoisoflavans.

The compound eluted at 13.9 min was identified to be urolithin C (**21**) (m/z 243, $[M - H]^-$, Figure 3e). Usually, it has been referred to as compound-type C, and its identity has been determined recently based on LC-ESI MS/MS, GC-MS, and NMR studies [36]. Since the structure of urolithin C is stabilized by resonance, the initiation of its fission required higher collision energies, and the fragmentation mostly led to the detachment of small molecules, such as OH (m/z 226), CO (m/z 215), CH₂O (m/z 213), CO₂ (m/z 199), and double CO (m/z 187).

2.1.5. Logwood

Chromatograms acquired using spectrophotometric detection for the logwood extract showed several not-very-intense peaks at shorter retention times (Figure 1h). Two of them were identified to be hematein (**1**) and hematoxylin (**2**), a brazilin-type homoisoflavonoid [43]. Their MS/MS spectra (Supplementary Materials, Figure S7) showed that the decomposition of hematoxylin occurred via a D-ring, whereas hematein fragmented by the fission of a heterocyclic C-ring. Proposed fragmentation pathways are shown in Supplementary Materials, Figure S8.

The next four compounds observed in the chromatogram were found to be potential logwood markers (Supplementary Materials, Figure S9). The first two of them, coded as hc1 (**4**) and hc2 (**10**), were eluted at 5.8 min ($[M - H]^-$ at m/z 319 \rightarrow 259, 247, 241, 227) and 8.2 min ($[M - H]^-$ at m/z 317 \rightarrow 195, 167, 152, 125), respectively, but their structures have not been established. The other two compounds eluting at 7.2 min ($[M - H]^-$ at m/z 603 \rightarrow 301, 179, 137) and 9.4 min ($[M - H]^-$ at m/z 581 \rightarrow 281) were coded as hc3 (**7**) and hc4 (**15**), respectively. The higher m/z values of their quasi-molecular ions, low fragmentation, and generated product ions suggested these compounds could be a combined structure of two colorants. Therefore, since the product ions acquired for hc3 corresponded to the quasi-molecular and product ions of hematoxylin, hc3 (**7**) was considered to be a hematoxylin dimer.

2.1.6. Sandalwood

Chromatograms acquired by a UV-Vis detector at 400 or 500 nm for the sandalwood extract showed four intense peaks (Figure 1i). According to the literature [44], it should contain santalins and santarubins, which was confirmed by MS/MS data. The first compound (t_R 27.6 min), identified to be santalin A (**62**), gave the $[M - H]^-$ ion at m/z 581 and its fragments at m/z 566, 551, and 523 (Figure 2f) corresponding to the single or double loss of CH₃ radicals from methoxy groups and to the further detachment of CO from a carbonyl group, respectively.

Similar fragmentation pathways were observed for santalin B (**68**) (t_R 29.8 min, $[M - H]^-$ at m/z 595, Figure 2g) and santarubin A (**74**) (t_R 30.9 min, $[M - H]^-$ at m/z 609, Figure 2h). Their MS/MS spectra showed ions $[M - H - CH_3]^-$ at m/z 580 and 594, $[M - H - 2CH_3]^-$ at m/z 565 and 579, $[M - H - 3CH_3]^-$ at m/z 550 and 564, and $[M - H - 2CH_3 - CO]^-$ at m/z 537 and 551, respectively. Moreover, in the santalin B (**68**) spectra, there was also an intense signal at m/z 547 corresponding to the loss of H₂O and two CH₃ moieties.

The fragmentation of the last compound (t_R 30.2 min, $[M - H]^-$ at m/z 503, Supplementary Materials, Figure S10), which was coded as ps1 (**71**), proceeded according to the same pattern (m/z 488 $[M - H - CH_3]^-$, 473 $[M - H - 2CH_3]^-$, and 445 $[M - H - 2CH_3 - CO]^-$), but the acquired MS/MS spectra turned out to be insufficient for determining the structure of the compound.

2.1.7. Orchil

The chromatogram acquired in positive full scan mode by the ESI MS detector for the extract of wool dyed with orchil (*Rocella tinctoria* DC.) showed three significant as well as six minor peaks. According to the available literature data, these compounds corresponded to aminoorceins. To confirm the identity, the MS/MS spectra were acquired.

The most intense peak present in the chromatogram (Figure 1j) at 22.7 min was identified to be α -aminoorcein (49) ($[M + H]^+$ at m/z 363). On the basis of the literature and by analogy with α -aminoorcein, it was assumed that the other two minor peaks corresponded to α -aminoorceinimine (45) ($[M + H]^+$ at m/z 362) and α -hydroxyorcein (58) ($[M + H]^+$ at m/z 364). Product ion spectra acquired by a triple-quadrupole mass spectrometer for the precursor ions of all three α -orceins indicated far-reaching similarity. Nonetheless, the identity of the MS/MS signals and determination of the fragmentation paths were very difficult, as most neutral losses could not be positively determined without high-resolution data due to the variety of possible isobaric fragments. For example, the loss of 17 Da could correspond to OH or NH₃, whereas the loss of 29 Da could correlate with the detachment of CHO, C₂H₅, CH₂N, or CH₂NH. Since these losses are indistinguishable by triple quadrupole MS, the orchil extract was next examined using quadrupole-time-of-flight tandem mass spectrometry (QToF MS). High-resolution and high-accuracy product ions are presented in Table 2.

Table 2. Product ions acquired using high-resolution MS/MS for protonated ions of orceins extracted from wool dyed with orchil.

Compound	t_R , min	$[M + H]^+$, m/z	Fragment ion, m/z	Calc. m/z	Formula	Diff, ppm	Abund %
β/γ -aminoorcein (32)	17.2	485.1718	470.1478	485.1707	C ₂₈ H ₂₅ N ₂ O ₆	-2.20	100.0
			469.1526	470.1472	C ₂₇ H ₂₂ N ₂ O ₆	-1.24	90.3
			468.1679	469.1520	C ₂₈ H ₂₃ NO ₆	-1.36	45.4
			467.1615	468.1680	C ₂₈ H ₂₄ N ₂ O ₅	0.21	57.0
			457.1760	467.1602	C ₂₈ H ₂₃ N ₂ O ₅	-2.91	16.4
			453.1453	457.1758	C ₂₇ H ₂₅ N ₂ O ₅	-0.51	14.1
			425.1242	453.1445	C ₂₇ H ₂₁ N ₂ O ₅	-1.86	34.2
			415.1653	425.1258	C ₂₆ H ₁₉ NO ₅	3.79	25.7
			414.1571	415.1652	C ₂₅ H ₂₃ N ₂ O ₄	-0.18	69.5
			400.1436	414.1574	C ₂₅ H ₂₂ N ₂ O ₄	0.82	23.8
			399.1367	400.1418	C ₂₄ H ₂₀ N ₂ O ₄	-4.52	36.3
			387.1694	399.1339	C ₂₄ H ₁₉ N ₂ O ₄	-6.89	26.1
			371.1389	387.1703	C ₂₄ H ₂₃ N ₂ O ₃	2.26	23.9
			362.1262	371.1390	C ₂₃ H ₁₉ N ₂ O ₃	0.22	18.8
			347.1383	362.1261	C ₂₁ H ₁₈ N ₂ O ₄	-0.43	26.2
			347.1021	347.1390	C ₂₁ H ₁₉ N ₂ O ₃	2.17	10.9
			334.1303	347.1026	C ₂₀ H ₁₅ N ₂ O ₄	1.45	12.9
			333.1245	334.1312	C ₂₀ H ₁₈ N ₂ O ₃	2.60	10.2
			283.1083	333.1234	C ₂₀ H ₁₇ N ₂ O ₃	-3.35	16.6
				283.1077	C ₁₆ H ₁₅ N ₂ O ₃	-2.09	7.5
β/γ -aminoorceinimine (33)	17.3	484.1869	469.1633	484.1867	C ₂₈ H ₂₆ N ₃ O ₅	-0.40	100.0
			468.1669	469.1632	C ₂₇ H ₂₃ N ₃ O ₅	-0.20	76.6
			467.1836	468.1680	C ₂₈ H ₂₄ N ₂ O ₅	2.25	73.1
			467.1615	467.1840	C ₂₈ H ₂₅ N ₃ O ₄	0.78	23.4
			466.1789	467.1602	C ₂₈ H ₂₃ N ₂ O ₅	-2.97	22.5
			453.1430	466.1761	C ₂₈ H ₂₄ N ₃ O ₄	-5.95	14.0
			424.1408	453.1445	C ₂₇ H ₂₁ N ₂ O ₅	3.27	43.9
			415.1658	424.1418	C ₂₆ H ₂₀ N ₂ O ₄	2.32	27.5
			414.1585	415.1652	C ₂₅ H ₂₃ N ₂ O ₄	-1.28	46.4
			400.1685	414.1574	C ₂₅ H ₂₂ N ₂ O ₄	-2.63	21.0
			387.1724	400.1656	C ₂₄ H ₂₂ N ₃ O ₃	-7.33	27.4
			361.1419	387.1703	C ₂₄ H ₂₃ N ₂ O ₃	-5.30	19.1
			346.1209	361.1421	C ₂₁ H ₁₉ N ₃ O ₃	0.63	23.2
				346.1186	C ₂₀ H ₁₆ N ₃ O ₃	-6.65	21.9
			β/γ -hydroxyorcein (44)	21.7	486.1561	471.1309	486.1547
470.1231	471.1313	C ₂₇ H ₂₁ NO ₇				0.87	100.0
469.1515	470.1234	C ₂₇ H ₂₀ NO ₇				0.57	16.9
468.1450	469.1520	C ₂₈ H ₂₃ NO ₆				1.13	59.1
458.1590	468.1442	C ₂₈ H ₂₂ NO ₆				-1.69	20.8
454.1285	458.1598	C ₂₇ H ₂₄ NO ₆				1.77	16.1
440.1488	454.1285	C ₂₇ H ₂₀ NO ₆				-0.07	35.6
425.1266	440.1493	C ₂₇ H ₂₂ NO ₅				1.05	13.6
416.1491	425.1258	C ₂₆ H ₁₉ NO ₅				-1.81	37.2
415.1421	416.1493	C ₂₅ H ₂₂ NO ₅				0.58	63.6
	415.1414	C ₂₅ H ₂₁ NO ₅				-1.66	30.6

Table 2. Cont.

Compound	t_R , min	$[M + H]^+$, m/z	Fragment ion, m/z	Calc. m/z	Formula	Diff, ppm	Abund %
			401.1258	401.1258	C ₂₄ H ₁₉ NO ₅	-0.10	37.4
			400.1185	400.1179	C ₂₄ H ₁₈ NO ₅	-1.37	23.3
			388.1544	388.1543	C ₂₄ H ₂₂ NO ₄	-0.15	40.2
			386.1010	386.1023	C ₂₃ H ₁₆ NO ₅	3.37	12.2
			384.1234	384.1204	C ₂₁ H ₂₀ O ₇	-7.71	12.5
			373.1311	373.1309	C ₂₃ H ₁₉ NO ₄	-0.40	21.9
			372.1236	372.1230	C ₂₃ H ₁₈ NO ₄	-1.64	12.8
			363.1113	363.1101	C ₂₁ H ₁₇ NO ₅	-3.28	33.5
			348.0864	348.0866	C ₂₀ H ₁₄ NO ₅	0.57	19.3
			346.1429	346.1438	C ₂₂ H ₂₀ NO ₃	2.57	15.8
			334.1078	334.1074	C ₂₀ H ₁₆ NO ₄	-1.11	25.9
			293.1053	293.1046	C ₁₈ H ₁₅ NO ₃	-2.46	17.3
			264.1032	264.1019	C ₁₇ H ₁₄ NO ₂	-4.96	14.4
α -aminoorcinimine (45)	21.9	362.1499		362.1499	C ₂₁ H ₂₀ N ₃ O ₃	-0.08	100.0
			347.1264	347.1264	C ₂₀ H ₁₇ N ₃ O ₃	0.04	73.8
			346.1318	346.1312	C ₂₁ H ₁₈ N ₂ O ₃	-1.85	47.4
			345.1461	345.1472	C ₂₁ H ₁₉ N ₃ O ₂	4.01	19.2
			345.1230	345.1234	C ₂₁ H ₁₇ N ₂ O ₃	1.19	10.3
			344.1391	344.1394	C ₂₁ H ₁₈ N ₃ O ₂	0.81	17.6
			332.1031	332.1030	C ₁₉ H ₁₄ N ₃ O ₃	-0.42	19.7
			331.1078	331.1077	C ₂₀ H ₁₅ N ₂ O ₃	-0.27	33.1
			330.1245	330.1237	C ₂₀ H ₁₆ N ₃ O ₂	-2.39	38.3
			302.1047	302.1050	C ₁₉ H ₁₄ N ₂ O ₂	0.93	26.3
			293.1297	293.1284	C ₁₈ H ₁₇ N ₂ O ₂	-4.26	17.5
			278.1283	278.1288	C ₁₇ H ₁₆ N ₃ O	1.62	24.0
			264.1140	264.1131	C ₁₆ H ₁₄ N ₃ O	-3.41	12.0
			262.1099	262.1101	C ₁₇ H ₁₄ N ₂ O	0.76	9.3
			239.1055	239.1053	C ₁₄ H ₁₃ N ₃ O	-0.80	30.4
β/γ -aminoorcinimine (46)	22.0	484.1868		484.1867	C ₂₈ H ₂₆ N ₃ O ₅	-0.28	100.0
			469.1629	469.1632	C ₂₇ H ₂₅ N ₃ O ₅	0.60	61.5
			468.1668	468.1680	C ₂₈ H ₂₄ N ₂ O ₅	2.58	71.4
			467.1783	467.1840	C ₂₈ H ₂₅ N ₃ O ₄	12.18	17.6
			466.1775	466.1761	C ₂₈ H ₂₄ N ₃ O ₄	-3.05	11.1
			453.1436	453.1445	C ₂₇ H ₂₁ N ₂ O ₅	1.94	26.5
			452.1613	452.1605	C ₂₇ H ₂₂ N ₃ O ₄	-1.70	25.1
			424.1422	424.1418	C ₂₆ H ₂₀ N ₂ O ₄	-0.94	17.8
			415.1630	415.1652	C ₂₅ H ₂₃ N ₂ O ₄	5.30	16.6
			400.1664	400.1656	C ₂₄ H ₂₂ N ₃ O ₃	-2.05	12.5
			361.1429	361.1421	C ₂₁ H ₁₉ N ₃ O ₃	-2.10	24.1
			346.1196	346.1186	C ₂₀ H ₁₆ N ₃ O ₃	-2.83	8.2
β/γ -aminoorcin (47)	22.3	485.1721		485.1707	C ₂₈ H ₂₅ N ₂ O ₆	-2.94	100.0
			470.1473	470.1472	C ₂₇ H ₂₂ N ₂ O ₆	-0.30	86.1
			469.1511	469.1520	C ₂₈ H ₂₃ NO ₆	1.83	35.2
			468.1681	468.1880	C ₂₈ H ₂₄ N ₂ O ₅	-0.21	53.5
			467.1602	467.1602	C ₂₈ H ₂₃ N ₂ O ₅	-0.06	14.5
			457.1762	457.1758	C ₂₇ H ₂₅ N ₂ O ₅	-0.87	15.7
			453.1442	453.1445	C ₂₇ H ₂₁ N ₂ O ₅	0.73	29.4
			425.1266	425.1258	C ₂₆ H ₁₉ NO ₅	-1.79	20.7
			415.1657	415.1652	C ₂₅ H ₂₃ N ₂ O ₄	-1.28	63.2
			414.1575	414.1574	C ₂₅ H ₂₂ N ₂ O ₄	-0.17	21.0
			400.1412	400.1418	C ₂₄ H ₂₀ N ₂ O ₄	1.50	34.6
			399.1371	399.1339	C ₂₄ H ₁₉ N ₂ O ₄	-7.97	22.0
			387.1697	387.1703	C ₂₄ H ₂₃ N ₂ O ₃	1.58	28.0
			371.1387	371.1390	C ₂₃ H ₁₉ N ₂ O ₃	0.86	14.9
			362.1262	362.1261	C ₂₁ H ₁₈ N ₂ O ₄	-0.30	22.5
			347.1375	347.1390	C ₂₁ H ₁₉ N ₂ O ₃	4.26	7.6
			347.1022	347.1026	C ₂₀ H ₁₅ N ₂ O ₄	1.24	19.5
			334.1302	334.1312	C ₂₀ H ₁₈ N ₂ O ₃	2.90	9.0
			333.1238	333.1234	C ₂₀ H ₁₇ N ₂ O ₃	-1.17	12.0
			283.1068	283.1077	C ₁₆ H ₁₅ N ₂ O ₃	3.21	4.4
α -aminoorcin (49)	22.7	363.1342		363.1339	C ₂₁ H ₁₉ N ₂ O ₄	-0.73	75.2
			348.1106	348.1105	C ₂₀ H ₁₆ N ₂ O ₄	-0.41	100.0
			347.1145	347.1152	C ₂₁ H ₁₉ N ₂ O ₄	2.06	58.7
			346.1298	346.1312	C ₂₁ H ₁₈ N ₂ O ₃	3.93	30.1
			346.1063	346.1074	C ₂₁ H ₁₆ NO ₄	3.01	11.0
			345.1232	345.1234	C ₂₁ H ₁₇ N ₂ O ₃	0.41	18.8
			335.1400	335.1400	C ₂₀ H ₁₉ N ₂ O ₃	-2.78	2.3
			333.0876	333.0870	C ₁₉ H ₁₃ N ₂ O ₄	-1.81	19.1
			332.0918	332.0917	C ₂₀ H ₁₄ NO ₄	-0.21	46.7
			331.1063	331.1077	C ₂₀ H ₁₅ N ₂ O ₃	4.14	42.1
			330.1108	330.1125	C ₂₁ H ₁₆ NO ₃	5.03	21.2
			303.0900	303.0890	C ₁₉ H ₁₃ NO ₃	-3.35	67.2
			293.1289	293.1285	C ₁₈ H ₁₇ N ₂ O ₂	-1.39	4.8
			292.1209	292.1206	C ₁₈ H ₁₆ N ₂ O ₂	-0.83	9.5
			279.1128	279.1128	C ₁₇ H ₁₅ N ₂ O ₂	0.03	27.5
			265.0969	265.0969	C ₁₆ H ₁₃ N ₂ O ₂	0.80	7.4
			240.0892	240.0893	C ₁₄ H ₁₂ N ₂ O ₂	0.43	51.9

Table 2. Cont.

Compound	t_R , min	$[M + H]^+$, m/z	Fragment ion, m/z	Calc. m/z	Formula	Diff, ppm	Abund %			
β/γ -hydroxyorcein (56)	26.6	486.1548	471.1310	486.1547	$C_{28}H_{24}NO_7$	-0.31	40.7			
			471.1313	471.1313	$C_{27}H_{21}NO_7$	0.63	100.0			
			469.1517	469.1520	$C_{28}H_{23}NO_6$	0.52	74.3			
			468.1438	468.1442	$C_{28}H_{22}NO_6$	0.82	23.3			
			458.1594	458.1598	$C_{27}H_{24}NO_6$	0.90	22.6			
			454.1285	454.1285	$C_{27}H_{20}NO_6$	0.09	41.9			
			440.1501	440.1493	$C_{27}H_{22}NO_5$	-2.00	12.9			
			425.1246	425.1258	$C_{26}H_{19}NO_5$	2.77	28.8			
			416.1487	416.1493	$C_{25}H_{22}NO_5$	1.31	83.8			
			401.1259	401.1258	$C_{24}H_{19}NO_5$	-0.22	45.8			
			400.1187	400.1179	$C_{24}H_{18}NO_5$	-1.91	28.1			
			388.1543	388.1543	$C_{24}H_{22}NO_4$	-0.02	43.8			
			384.1189	384.1204	$C_{21}H_{20}O_7$	3.72	17.1			
			373.1306	373.1309	$C_{23}H_{19}NO_4$	0.75	13.7			
			372.1236	372.1230	$C_{23}H_{18}NO_4$	-1.45	13.5			
			363.1104	363.1101	$C_{21}H_{17}NO_5$	-0.87	13.8			
			348.0860	348.0866	$C_{20}H_{14}NO_5$	1.95	14.0			
			346.1432	346.1438	$C_{22}H_{20}NO_3$	1.67	22.0			
			334.1068	334.1074	$C_{20}H_{16}NO_4$	1.79	24.1			
			292.0975	292.0968	$C_{18}H_{14}NO_3$	-2.17	9.5			
			264.1015	264.1019	$C_{17}H_{14}NO_2$	1.72	13.9			
			α -hydroxyorcein (58)	27.3	364.1184	349.0946	364.1179	$C_{21}H_{18}NO_5$	-1.17	30.9
						349.0945	349.0945	$C_{20}H_{15}NO_5$	-0.45	79.6
						348.0867	348.0866	$C_{20}H_{14}NO_5$	-0.10	29.5
						347.1152	347.1152	$C_{21}H_{17}NO_4$	-0.07	45.6
						346.1079	346.1074	$C_{21}H_{16}NO_4$	-1.60	40.5
336.1232	336.1230	$C_{20}H_{18}NO_4$				-0.49	15.1			
334.0717	334.0710	$C_{19}H_{12}NO_5$				-2.12	8.8			
332.0919	332.0917	$C_{20}H_{14}NO_4$				-0.43	55.3			
331.0841	331.0839	$C_{20}H_{13}NO_4$				-0.49	38.9			
318.1132	318.1125	$C_{20}H_{16}NO_3$				-2.32	16.2			
303.0897	303.0890	$C_{19}H_{13}NO_3$				-2.22	54.6			
294.1126	294.1125	$C_{18}H_{16}NO_3$				-0.34	100.0			
293.1049	293.1046	$C_{18}H_{15}NO_3$				-0.95	37.8			
279.0892	279.0890	$C_{17}H_{13}NO_3$				-0.57	81.4			
266.1173	266.1176	$C_{17}H_{16}NO_2$				0.98	57.6			
266.0816	266.0816	$C_{16}H_{12}NO_3$				-1.69	8.0			
251.0938	251.0941	$C_{16}H_{13}NO_2$				1.22	30.5			
250.0868	250.0863	$C_{16}H_{12}NO_2$				-2.33	25.9			
241.0736	241.0733	$C_{14}H_{11}NO_3$				-0.96	25.9			
226.0862	226.0863	$C_{14}H_{12}NO_2$				0.21	16.4			
212.0706	212.0706	$C_{13}H_{10}NO_2$				0.27	38.9			

High-accuracy measurements of the $[M + H]^+$ ions and the formulas calculated on their basis—that is, m/z 363.1342: $C_{21}H_{19}N_2O_4$; 362.1499: $C_{21}H_{19}N_3O_3$; and 364.1179: $C_{21}H_{17}NO_5$ —corresponded to α -aminoorcein (49), α -aminoorceinimine (45), and α -hydroxyorcein (58), respectively. Since these colorants are stabilized by their resonance structures, clear and legible MS/MS spectra were acquired only using higher collision energy (CE) values, such as 30–45 V (Figure 4), and the fragmentations started from the detachments of small radicals. Although thermodynamic arguments preclude the possibility of the loss of radicals from even-electron ions, the high-resolution mass spectra of orceins contradict this generally known theory. The most intense signals (at m/z 348.1106, 347.1264, and 349.0946 for α -aminoorcein, α -aminoorceinimine, and α -hydroxyorcein, respectively) corresponded to the loss of CH_3 . Except that, the $[M + H - OH]^+$ ions were also present (m/z 346.1298, 345.1461, and 347.1152), but their origin was probably twofold. On the one hand, the hydroxyl radical could be detached from one of the two hydroxyl substituents of a phenyl ring (Figure 5). The same loss might also be achieved for α -hydroxyorcein by the homolytic cleavage of the hydroxyl group at the C-7 position of phenoxazin-3-one (m/z 347.1152). Since the other two compounds, α -aminoorcein and α -aminoorceinimine, are substituted at the C-7 position by an amino group, the detachment of the C-7 substituent led to the loss of an aminyl radical (NH_2) and the formation of the m/z 347.1145 and 346.1318 ions, respectively. Even though radical loss from even-electron ions is rather unusual, this phenomenon has been already observed for prodiginines used as inks [45].

The fragmentation path also included the loss of small neutral fragments, such as H_2O and CH_4 . It was observed mainly in the spectra of α -hydroxyorcein (m/z 348.0867) though, but the signals were less intense than those corresponding to the loss of radicals. The elimination of methane probably occurred between two methyl groups at the C-6 and C-9 positions, leading to the formation of the

inner cyclopentadiene ring between the phenyl substituent and phenoxazin-3-one structure. A similar mechanism was responsible for the elimination of H₂O from α -aminoorcein and α -hydroxyorcein (m/z 345.1232 and 346.1079, respectively) as well as of NH₃ from α -aminoorceinimine (m/z 345.1230). These losses occurred between the C-2-hydroxyl group of the phenyl moiety and the C-7 substituent of the phenoxazine skeleton. Moreover, due to the presence of a carbonyl group at the C-3 position of α -aminoorcein and α -hydroxyorcein, one of the possible fragmentation paths also led to the detachment of the CO molecule (the m/z 335.1400 and 336.1232 ions, respectively), which was not observed for α -aminoorceinimine (Figure 5).

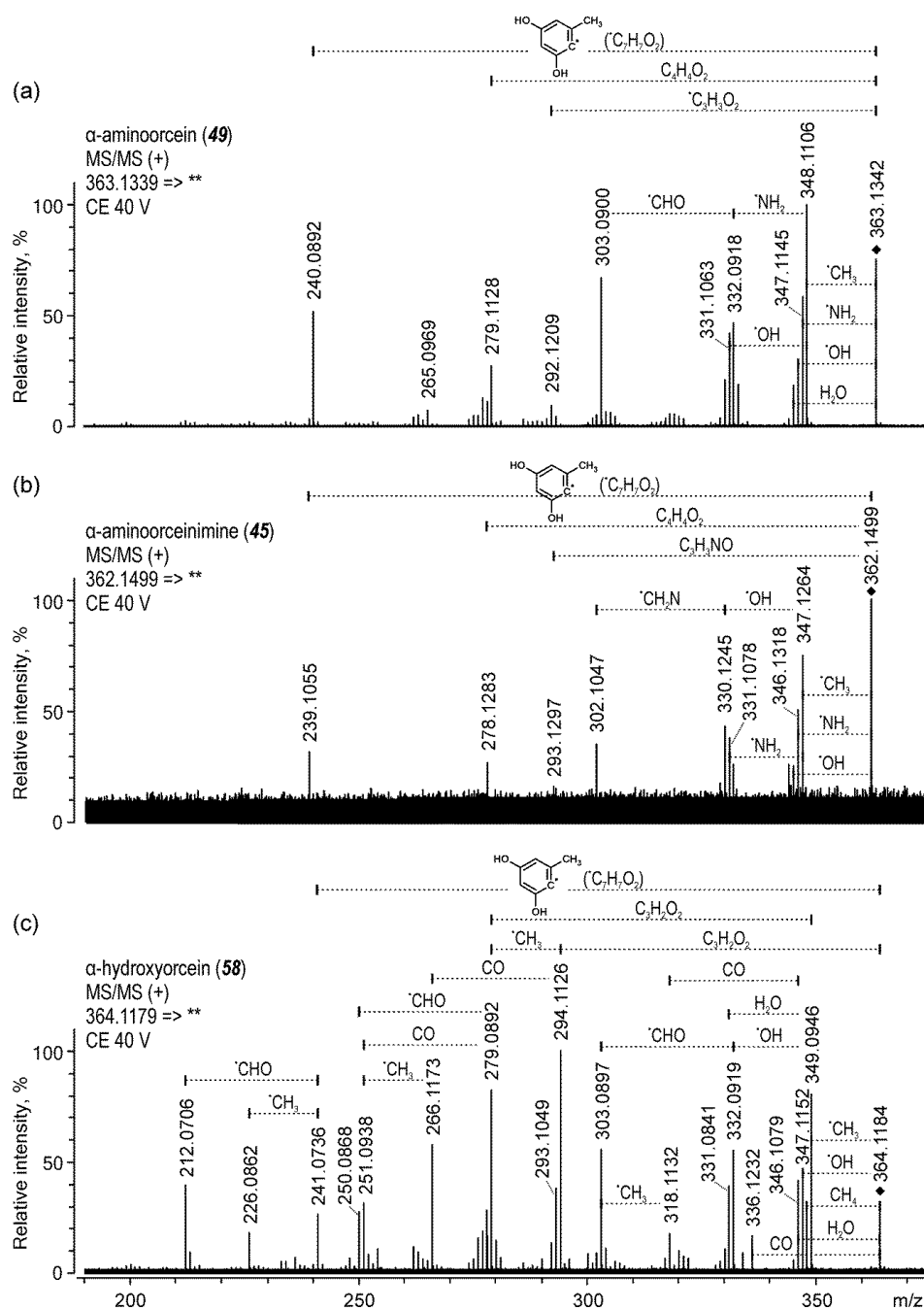


Figure 4. High resolution MS/MS spectra acquired in positive ion mode for α -aminoorcein (a), α -aminoorceinimine (b), and α -hydroxyorcein (c).

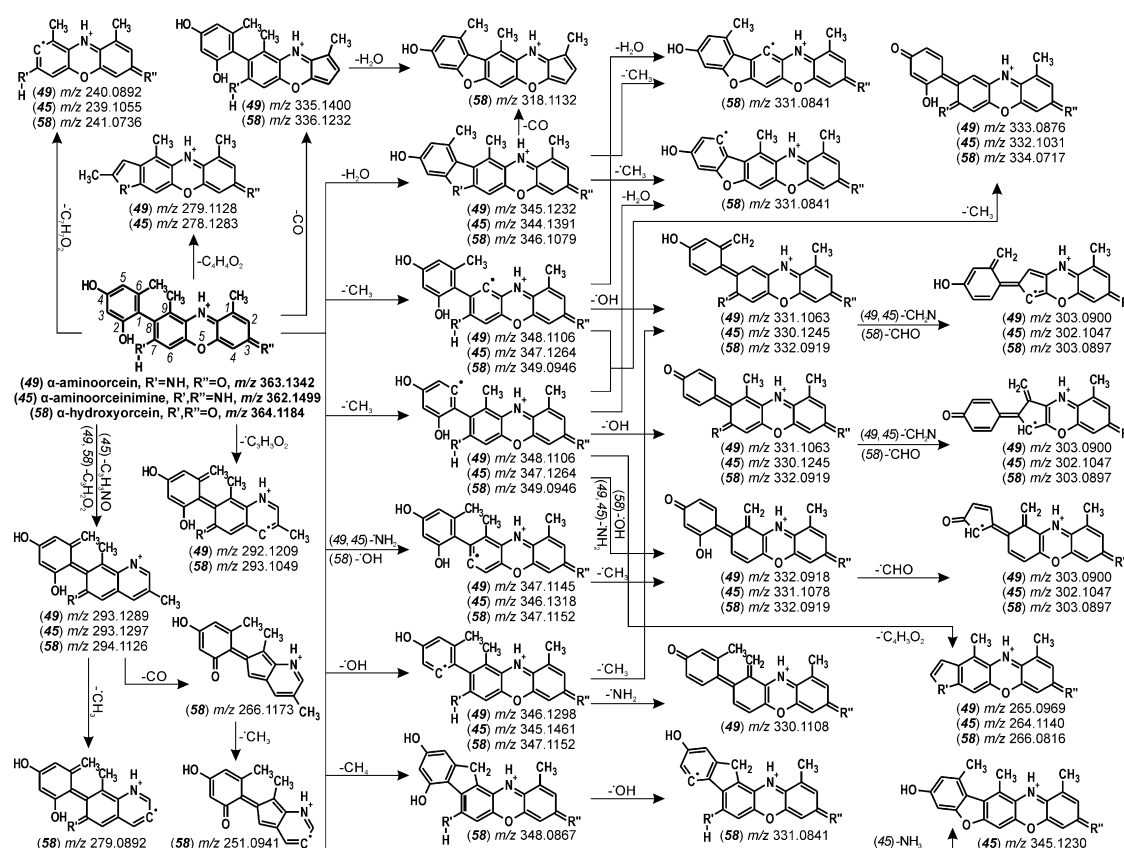


Figure 5. Proposed fragmentation pathways for α -aminoorcein (49), α -aminoorceinimine (45), and α -hydroxyorcein (58).

The next fragmentation stage was the further loss of the same small molecules (neutral and radical) from the primary product ions. The MS/MS spectra also showed the elimination of CHO or CH_2N within the hydroxyl substituents or the amino group at the C-7 position of phenoxazine.

Apart from the loss of small neutrals or small radicals, the fragmentation of α -orceins also occurred with the detachment of larger fragments. One of them, the 2,4-dihydroxy-6-methylphenyl radical ($\text{C}_7\text{H}_7\text{O}_2$), was created via a homolytic cleavage of the C-C bond between the phenyl ring and phenoxazine skeleton. The signals corresponding to this loss were observed in the spectra of α -aminoorcein, α -aminoorceinimine, and α -hydroxyorcein at m/z 240.0892, 239.1055, and 241.0736, respectively. Other losses were a result of a cross-ring fission. The primary loss of CH_3 from the 2,4-dihydroxy-6-methylphenyl substituent probably triggered the ring fission and detachment of the $\text{C}_4\text{H}_3\text{O}_2$ radical that was followed by the furan or pyrrole ring formation. Moreover, analogous ion structures were created by the elimination of the $\text{C}_4\text{H}_4\text{O}_2$ molecules from the phenyl substituent, but these signals were present only in the MS/MS spectra of α -aminoorceinimine (m/z 278.1283) and α -aminoorcein (m/z 279.1128).

The next fragmentation path included the fission of the phenoxazine system and detachment of the structure between atoms 3 and 5. Since α -aminoorcein and α -hydroxyorcein are substituted at the C-3 position by a carbonyl group—and α -aminoorceinimine, by a primary ketimine group—this cleavage resulted in the loss of the $\text{C}_3\text{H}_2\text{O}_2$ or $\text{C}_3\text{H}_3\text{NO}$ molecules, respectively. In the case of α -hydroxyorcein, the $[\text{M} + \text{H} - \text{C}_3\text{H}_2\text{O}_2]^+$ ion (m/z 294.1126) was very intense, hence its further fragmentation and subsequent detachment of the CO molecule (m/z 266.1173) and CH_3 radical (m/z 279.0892). Moreover, the alternative fission of the phenoxazine-3-one skeleton also led to the loss of the $\text{C}_3\text{H}_3\text{O}_2$ fragment from quasi-molecular ions of α -aminoorcein and α -hydroxyorcein (giving the m/z 292.1209 and 293.1049 ions, respectively).

The peaks of three β - and three γ -orceins were also observed in the chromatogram, but since there were no significant differences between the MS/MS spectra of their β - and γ -isomers, distinction between their two forms was not possible. Moreover, peaks that corresponded to β - and γ -hydroxyorcein showed very low intensities.

Since β - and γ -orceins are substituted by two 2,4-dihydroxy-6-methylphenyl groups (at the C-2 and C-8 positions), their fragmentation generated more product ions than the fragmentation of α -orceins. Nevertheless, these ions were produced, similarly as for α -orceins, according to the three paths: (1) the loss of small molecules, (2) phenyl ring fission, and (3) phenoxazine system fission. Most ions, however, especially those acquired for β - and γ -aminoorceins and hydroxyorceins (Figure 6), were formed as a result of various combination of these three pathways. MS/MS spectra showed signals corresponding to ions of mixed origin, such as $[M + H - CH_3 - C_3H_2O_2]^+$, $[M + H - CH_3 - C_3H_3O_2]^+$, $[M + H - CO - C_3H_2O_2]^+$, $[M + H - CH_3 - C_7H_7O_2]^+$, and $[M + H - CHO - C_7H_7O_2]^+$ (or $[M + H - CO - C_3H_3NO]^+$ in the case of β - and γ -aminoorceinimine).

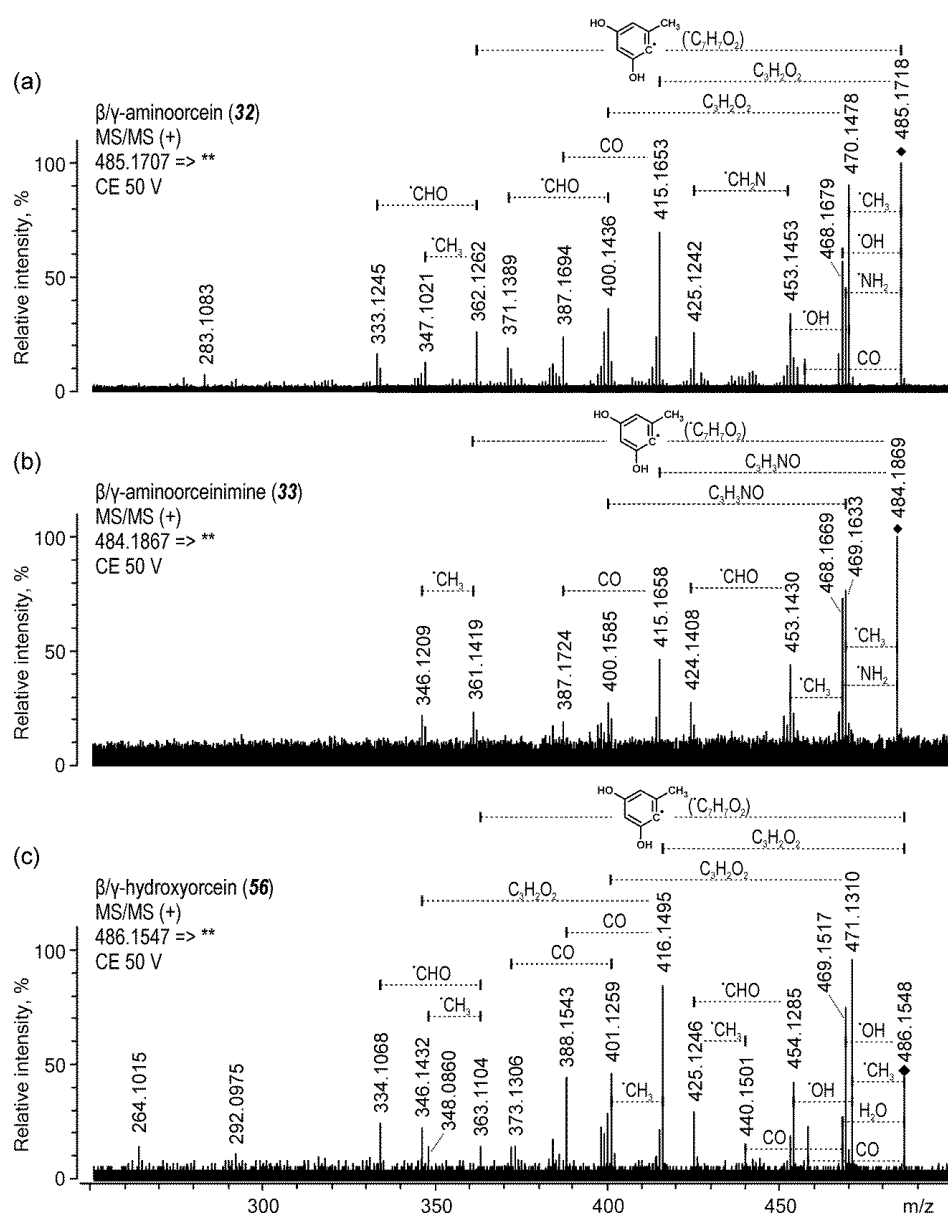


Figure 6. High-resolution MS/MS spectra acquired in negative ion mode for β/γ -aminoorcein (a), β/γ -aminoorceinimine (b), and β/γ -hydroxyorcein (c).

2.2. Protocol for Analyzing Historical Samples

The analytical protocol for the identification of natural dyes in historic textiles using HPLC coupled with UV-Vis and MS detections was proposed herein. This approach considered sample color (and thus also the extraction method), the UV-Vis and MS data acquired for the colorants (natural standards and markers in dyed fibers), and our expertise. Thus, according to the protocol (Figure 7), the detection of the colorants in the methanolic extracts from fibers should be conducted as follows: (I) yellow, orange, and black samples should be examined at 280 and 400 nm, in negative ion MS mode; (II) brown, blue, and green samples, at 280, 400, 550, and 600 nm, in both positive and negative ion MS modes; and (III) red and purple samples, at 280, 480, 550, and 600 nm, in both positive and negative ion MS modes; moreover, the DMSO extracts from (IV) brown, blue, green, and purple fibers should be analyzed at 550 and 600 nm, in positive ion MS mode. The protocol, recommended herein, was applied to identify the natural dyes used in historical samples, as described below.

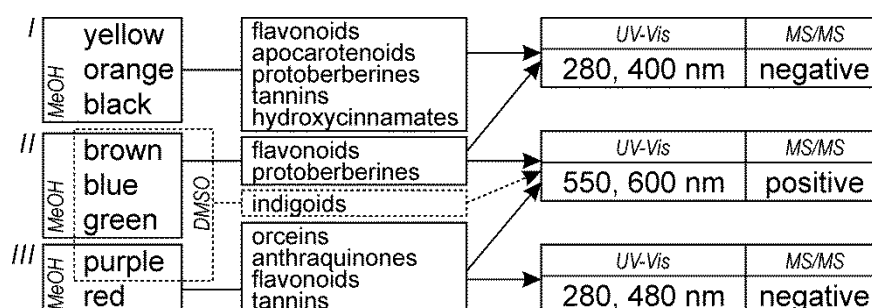


Figure 7. The integrated analytical protocol combining the extraction and analysis of colorants for the identification of natural dyes using HPLC-UV-Vis-ESI MS/MS.

2.3. Analysis of Historical Samples

The developed HPLC-UV-Vis-ESI MS/MS method was used to analyze 223 blue, purple, and red fibers taken from silk textiles dated from the 15th to 17th century and used in the vestments from the collections of twenty Krakow churches. The DMSO and methanol-water-formic acid extracts were analyzed using positive or positive and negative ion modes, respectively. The acquired results led to the identification of the natural dyes in the examined fibers, even though some of them were re-dyed with synthetic dyes. All the samples, identified colorants, and dyes are listed in Supplementary Materials, Table S1.

All the twenty-nine blue threads included in the set were dyed with indigo. Moreover, this dye was also identified in the next thirty-two samples of other colors (in fifteen at the trace level). Its use was proved by the presence of indigotin (65) in the extracts, always accompanied by isatin (13), a photodegradation product of indigotin. Indirubin was found only in some of these extracts. Since the composition of indigo colorants depends on the fermentation process for the indigo precursors, not on the origin of the plants used for this fermentation, indigo provenance could not be determined. Thus, the indigo could have been made from European or Asian plants from the genera *Indigofera*, *Isatis*, or others.

In 15th and 16th centuries, indigo was probably produced from woad (*Isatis tinctoria* L.), a native European plant that has been used on the Old Continent since antiquity. Although indigo from *Indigofera tinctoria* L. was imported to Europe after the discovery of the sea route to India, its use was much less likely at that time, since this dye was banned due to the allegedly “devilish origin” [46]. However, at the end of the 16th century, more and more Asian indigo came to Europe. Initially, it was used in combination with woad, but later on, during the 17th century, it replaced indigo from woad almost completely [44,46]. In consequence, threads taken from the younger textiles could be dyed using both *Indigofera* and *Isatis* species.

Although indigo was identified as a main dye in twenty-nine blue samples, it was used for individual dyeing in sixteen of them (in four of them, traces of other dyes were found as well). In another thirteen fibers, indigo was combined with other dyes and the fibers still remained blue. These dyes included American cochineal (one sample), weld (two samples), dyer's broom (one sample), and, above all, orchil (ten samples, in two of them, together with wild madder (Figure 8a)).

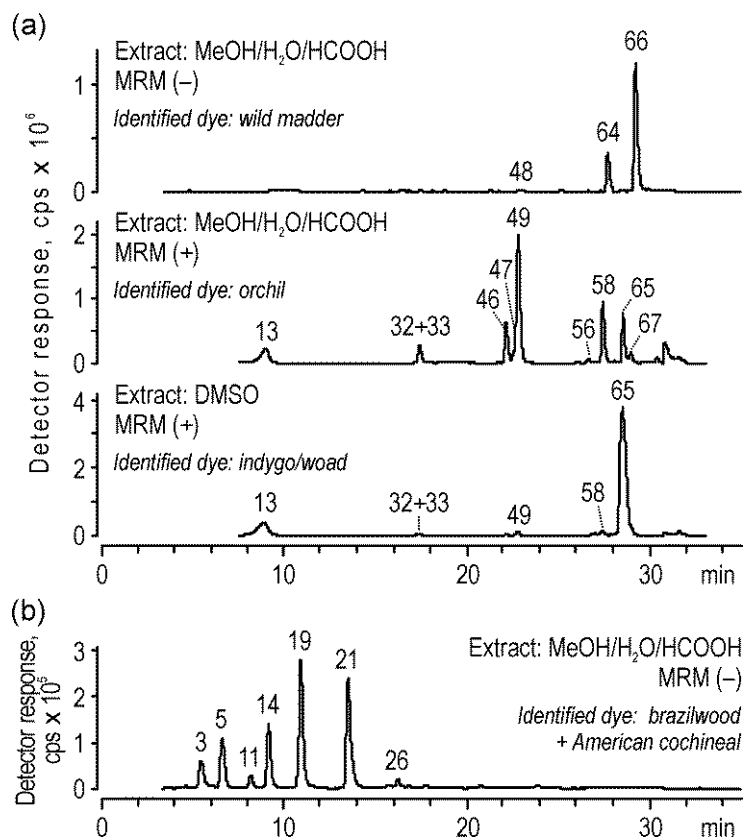


Figure 8. Chromatograms acquired for the extracts of the (a) blue sample (textile No. 282) and (b) red sample (textile No. 198) by the MS detector in negative and/or positive multiple reaction monitoring (MRM) modes; peak numbers are decoded in Table 1.

Orchil, as a red-purple direct dye produced from lichenized fungi in the genus *Rocella*, has been known in Europe since ancient times, but knowledge about its use was lost with the fall of the Western Roman Empire. The dye returned as a textile dye at the end of the 13th century and the beginning of the 14th century. Although its use was restricted in France in the second half of the 17th century due to its poor light resistance, it was still used in other European countries [46]. In consequence, orchil was identified in thirty-three blue, purple, and red fibers taken from 15th- to 17th-century textiles; this dye was always used in a mixture with other dyes, never individually.

Seven out of eight purple samples were dyed either with a combination of orchil and indigo or with a ternary mixture of orchil, indigo, and American cochineal. In one purple sample, orchil was not present at all. A mixture of indigo and American cochineal was used to achieve the intended color instead.

Kermes was identified in seven red threads, always together with orchil. All those samples were taken from 15th- to 16th-century European textiles. Polish (*Porphyrophora polonica* L.) or Armenian cochineal (*Porphyrophora hamelii* L.) were found in the next six samples dated to the same period, but the unequivocal determination of the dye was impossible, since both scale insects belong to the same genus and their compositions are very similar to each other. However, the largest group of samples was dyed with American cochineal (most likely *Dactylopius coccus* Costa), which after arriving to Europe in

1523 [44] quickly displaced from the market other red dyes of animal origin such as kermes and Polish and Armenian cochineals.

American cochineal was identified by the presence of carminic acid (19) together with minor colorants, such as dcII (18), dcIV (30), dcVII (36), carminic acid derivative (24), kermesic acid (52), and flavokermesic acid (51). Although similar compounds were also found for the samples dyed with *Porphyrophora* species, they stood out with clearly higher contents of flavokermesic acid (51) and kermesic acid (52) as well as a complete absence of dcII (18) and trace presence of pp12 (41), pp14 (53), and pp15 (60) instead. In consequence, American cochineal was found as the only dye in one hundred and one thread samples, whereas in the next eleven threads, it was used together with annatto, brazilwood, dyer's broom, and weld in single samples, as well as with indigo or its combination with orchil, as has already been mentioned. Nevertheless, most often, American cochineal was combined together with an unknown ellagitannin dye used as an organic mordant. These two dyes were identified together in eighteen samples.

The last identified animal-origin dye was lac dye (*Kerria lacca* Kerr or *K. chinensis* Mahdihassan). This Indian dye had been occasionally used in medieval Europe, but it gained popularity only in the second half of the 18th century [46]. Lac dye had been more widely known, however, in Muslim countries, including the Ottoman Empire, where it had been used to obtain crimson red. It was confirmed by the results, as lac dye was found in eight thread samples taken from 15th-century European textiles and in four fibers from 17th-century Turkish textiles.

The *Rubiaceae* dyes were identified in only nine samples (mostly dated to the 17th century); nevertheless, the different compositions of the anthraquinones in the extracts led to the distinguishing of three different chromatographic profiles. The first one, with high signals of alizarin (55), purpurin (64), and nordamnacanthal (72), corresponded to dyer's madder (*Rubia tinctorum* L.). It was observed only in two extracts, which is understandable considering that, although madder as a European plant was widely cultivated on the continent, it was mainly used for dyeing wool, not silk. A similar chromatographic profile but without the peak of nordamnacanthal indicated the use of the *Galium* species, which was probably used in one sample. The high signal of rubiadin (66) together with the almost complete absence of alizarin corresponded to wild madder (*Rubia peregrina* L.). This dye was mostly used together with orchil and indigo to produce purple shades (Figure 8a).

Red color was obtained not only using anthraquinone dyes but also with flavonoid dyes. Thus, eleven red threads were dyed with brazilwood, which was used both individually as well as in combination with American cochineal (Figure 8b) or annatto (results published in [37,38]). Moreover, brazilwood was also found in nine samples of other colors (mostly yellow and orange). The origin of dyes, however, could not be determined precisely, since the same colorants were obtained from different tree species. One of them, sappanwood (*Caesalpinia sappan* L.), from southern Asia, was already known and used in medieval Europe, wherein the inner part of its trunks was used to produce brazilwood. In later centuries, the dye was also obtained from species imported from South America, such as *Caesalpinia echinata* L. and *Haematoxylum brasiletto* Karst. Furthermore, these trees were used for dyeing not only red but also yellow and orange.

3. Materials and Methods

Carminic acid, ellagic acid, indigotin, isatin, and purpurin were purchased from Fluka (Buchs, Switzerland); anthrarufin, anthraflavic acid, chrysazine, chrysophanol, hematein, quinizarin, and rubiadin were purchased from Sigma-Aldrich (St. Louis, MO, USA); and alizarin and hematoxylin were purchased from Riedel-de Haën (Seelze, Germany). All the chemicals (except alizarin) were of analytical chemical grade. Indirubin had been synthesized earlier by Puchalska [4], and chromatographic purity was estimated by HPLC/DAD at 280 nm. Kermesic acid was kindly donated by Dr. Ioannis Karapanagiotis ("Ormylia" Art Diagnosis Centre, Ormylia, Greece).

Alum $\text{AlK}(\text{SO}_4)_2 \cdot 12\text{H}_2\text{O}$ of analytical grade was from POCH (Gliwice, Poland). Sheep wool came from a rural farm in the Kuczbork commune of Northern Mazovia (Kuczbork, Poland). Methanol

(LC/MS purity) and dimethyl sulfoxide (pure p.a.) were purchased from POCH (Gliwice, Poland); formic acid (LC/MS purity), from Fisher Scientific (Fair Lawn, NJ, USA); and hydrochloric acid (analytical grade, 35–38%), from AppliChem (Darmstadt, Germany). Demineralized water was made using a Milli-Q system Model Millipore Elix 3 (Molsheim, France).

Standard solutions of most colorants ($0.2 \text{ mg}\cdot\text{mL}^{-1}$) were prepared in methanol. Only indigotin and indirubin ($0.1 \text{ mg}\cdot\text{mL}^{-1}$) were dissolved in dimethyl sulfoxide (DMSO). Woolen yarns were mordanted, dyed, and extracted according to the procedure indicated previously [37]. Moreover, a 0.25 mg indigo sample was dissolved in 25 mL of DMSO. The solutions were kept in an ultrasonic bath for 5 min, and the obtained solutions was diluted 10 times with methanol.

The 223 silk fibers (red, purple, and blue) were taken from silk textiles that were dated to the 15th to 17th century and used in the vestments belonging to the collections of twenty Krakow churches (all the samples are listed in Supplementary Material, Table S1).

The purple and blue fibers were extracted twice, using two extraction methods consecutively, the first one with dimethylsulfoxide (DMSO), and the second one with acidic-methanol extractant. The red fibers were extracted only with the second procedure. The extraction procedures have been described in detail by Lech [37].

Chromatographic analyses were performed using a 1220 Infinity II LC System (Agilent Technologies, Waldbronn, Germany) with a Zorbax SB-Phenyl column ($4.6 \times 150 \text{ mm}$, $3.5 \mu\text{m}$, 80 \AA , Agilent Technologies); a Zorbax SB-Phenyl precolumn ($4.6 \times 12.5 \text{ mm}$, $5.0 \mu\text{m}$, Agilent Technologies); and a mixture of methanol, water, and formic acid as a mobile phase. Detection was carried out with a 1220 Compact Variable Wavelength Detector and a 1200 Variable Wavelength Detector (Agilent Technologies, Waldbronn, Germany), as well as with a 6460 Triple Quad LC/MS system with *JetStream* Technology (Agilent Technologies, Waldbronn, Germany). The full scan chromatograms and spectra were acquired for m/z 100–1000. Quasi-molecular ions of the colorants were fragmented using 15, 25, 35, and 45 V of collision energy (CE). The MS/MS spectra were acquired from m/z 50 to the m/z -value of the precursor ion + 20 to achieve an upper limit of around 20 m/z above the m/z of each fragmented ion. The parameters of the method were described in detail by Lech [37]. The final method was developed in dynamic multiple reaction monitoring (dMRM) mode given the most intense precursor and product ion pairs (transitions) of the identified dye markers. The optimal collision energy for each transition was selected manually. Detailed settings (the retention times, fragmentor values for each precursor ion, MRM transitions, and CEs of the new colorants) are provided in Table 1.

High-accuracy mass spectra of the natural orceins (phenoxazines) were acquired using a UHD Accurate-Mass 6540 Q-TOF LC/MS system with *JetStream* Technology (Agilent Technologies, USA). The MS was operated in positive ionization MS/MS mode. The following parameters were applied: probe voltage, 3500 V; nozzle voltage, 1000 V; gas temperature, $300 \text{ }^\circ\text{C}$; gas flow, $8 \text{ L}\cdot\text{min}^{-1}$; nebulizer pressure, 35 psig; sheath gas temperature, $350 \text{ }^\circ\text{C}$; sheath gas flow, $11 \text{ L}\cdot\text{min}^{-1}$; fragmentor, 120 V; collision energies, 30, 40, and 50 V; reference masses, m/z 121.05087300 and 922.00979800.

The analyses were performed using the MassHunter Workstation software (Agilent Technologies, USA).

4. Conclusions

A phenyl HPLC column and UV-Vis-ESI MS/MS technique were used to separate and characterize colorants (flavonoids, homoisoflavonoids, anthraquinones, indigoids, and orceins) present in the extracts of ten natural dyes (American cochineal, brazilwood, indigo, kermes, lac dye, logwood, madder, orchil, sandalwood, and Polish cochineal). Tandem mass spectrometric detection provided information on the structures of unknown colorants eluted from the HPLC column. Several colorants were identified in this way, including protosappanin B, protosappanin E, santalin A, santalin B, santarubin A, nordamnacanthal, lucidin, erythrolaccin, and deoxyerythrolaccin, but the structures of some compounds (from brazilwood, logwood, madder, and sandalwood) are still pending. Moreover, complex fragmentation pathways of α -, β - and γ - aminoorceins, hydroxyorceins, and aminoorceinimines

extracted from orchil-dyed wool have been defined the first time according to our knowledge on the basis of high-resolution mass spectrometry data acquired by QToF MS. The results have shown that the fragmentation is twofold. It occurs by the loss of small neutrals and radicals, as well as by the loss or fission of the aromatic rings.

MS/MS data have been used not only to identify new colorants but also to expand the existing dMRM method with 60 new dye markers. It has resulted in the development, as far as we know, of the first universal and comprehensive approach, that includes 176 colorants, intended for the identification of natural dyes in historical objects. Furthermore, a general analytical protocol has been developed for the identification of the natural dyes used in historical objects, antiques, and works of art. It involves both extraction and analysis steps (including UV-Vis detection wavelengths and MS ionization modes) and also considers fiber colors and the physicochemical properties of presumed dyes. This approach has been used to analyze 223 red, purple, and blue fibers taken from the silk textiles used in the vestments belonging to the collections of twenty Krakow churches. It has led to the identification of several dyes, such as orchil, brazilwood, madder, wild madder, indigo, lac dye, kermes, and different species of cochineals. The results of this study have completed the picture of natural dyes used in the most valuable textiles of European and Near Eastern origin dated to the 15th to 17th century.

Supplementary Materials: Figure S1: Indigo: MS/MS spectra of indigotin, indirubin, indigo compound A, and indigo compound A acquired in positive ion mode. Figure S2: Chemical structures of laccaic acids. Figure S3: Lac dye: MS/MS spectra of laccaic acid E, laccaic acid C, xantholaccaic acid B, laccaic acid B, xantholaccaic acid A, and laccaic acid A, acquired in negative ion mode. Figure S4: Madder: MS/MS spectra of rt1 (alizarin–lucidin dimer). Figure S5: Madder: MS/MS spectra of rubiadin *O*-primeveroside, ruberthyric acid, and lucidin *O*-primeveroside acquired in negative ion mode. Figure S6: Brazilwood: MS/MS spectra of brazilin-like compounds in negative ion mode. Figure S7: Logwood: MS/MS spectra of hematoxylin and hematein acquired in negative ion mode. Figure S8: Proposed fragmentation pathways for a) hematoxylin and b) hematein. Figure S9: Logwood: MS/MS spectra of hc1, hc2, hc3, and hc4 acquired in negative ion mode. Figure S10: Sandalwood: MS/MS spectra of santalin-like compound acquired in negative ion mode. Table S1. Compounds and dyes identified in silk textiles dated to the 15th to 17th century.

Author Contributions: K.L. designed the research, coordinated the work, carried out HPLC-UV-Vis-ESI MS/MS analysis, carried out data interpretation and discussions, and prepared the draft manuscript and drawings; E.F. carried out the UPLC-ESI QToF MS experiment. All authors have read and agreed to the published version of the manuscript.

Funding: This research was supported by the statutory fund of the Faculty of Chemistry, Warsaw University of Technology, Poland and by the Ministry of Science and Higher Education, Poland (grant no: 0008/NPRH3/H11/82/2014).

Acknowledgments: The authors would like to thank Perlan Technologies Polska (Warsaw, Poland) for the opportunity to conduct research using 1220 Infinity II LC Systems (Agilent Technologies), the Partnership Laboratory of the Warsaw Biological and Chemical Research Centre of Warsaw University, Agilent Technologies, and Tomasz Gromulski for the opportunity to conduct research using UPLC-ESI QToF MS. The authors would like to express their gratitude to Dominique Cardon (CNRS Laboratoire d'Histoire et d'Archéologie, Lyons, France), Dr. Natalia Krupa (Pontifical University of John Paul II, Krakow, Poland), and Ewa Soszko (Asia and Pacific Museum, Warsaw, Poland) for kindly donating samples.

Conflicts of Interest: The authors declare no conflict of interest.

References

1. Pauk, V.; Barták, P.; Lemr, K. Characterization of natural organic colorants in historical and art objects by high-performance liquid chromatography. *J. Sep. Sci.* **2014**, *37*, 3393–3410. [[CrossRef](#)] [[PubMed](#)]
2. Degano, I.; Ribechini, E.; Modugno, F.; Colombini, M.P. Analytical methods for the characterization of organic dyes in artworks and in historical textiles. *Appl. Spectrosc. Rev.* **2009**, *44*, 363–410. [[CrossRef](#)]
3. Surowiec, I. Application of high-performance separation techniques in archaeometry. *Microchim. Acta.* **2008**, *162*, 289–302. [[CrossRef](#)]
4. Puchalska, M.; Polec-Pawlak, K.; Zadrozna, I.; Hryszko, H.; Jarosz, M. Identification of indigoid dyes in natural organic pigments used in historical art objects by high-performance liquid chromatography coupled to electrospray ionization mass spectrometry. *J. Mass Spectrom.* **2004**, *39*, 1441–1449. [[CrossRef](#)] [[PubMed](#)]

5. Pawlak, K.; Puchalska, M.; Miszczak, A.; Rosłonec, E.; Jarosz, M. Blue natural organic dyestuffs—Front textile dyeing to mural painting. Separation and characterization of coloring matters present in elderberry, logwood and indigo. *J. Mass Spectrom.* **2006**, *41*, 613–622. [[CrossRef](#)] [[PubMed](#)]
6. Surowiec, I.; Szostek, B.; Trojanowicz, M. HPLC-MS of anthraquinoids, flavonoids, and their degradation products in analysis of natural dyes in archeological objects. *J. Sep. Sci.* **2007**, *30*, 2070–2079. [[CrossRef](#)]
7. Degano, I.; Biesaga, M.; Colombini, M.P.; Trojanowicz, M. Historical and archaeological textiles: An insight on degradation products of wool and silk yarns. *J. Chromatogr. A* **2011**, *1218*, 5837–5847. [[CrossRef](#)]
8. Lech, K.; Jarosz, M. Novel methodology for the extraction and identification of natural dyestuffs in historical textiles by HPLC-UV-Vis-ESI MS. Case study: Chasubles from the Wawel Cathedral collection. *Anal. Bioanal. Chem.* **2011**, *399*, 3241–3251. [[CrossRef](#)]
9. Mantzouris, D.; Karapanagiotis, I.; Valianou, L.; Panayiotou, C. HPLC-DAD-MS analysis of dyes identified in textiles from Mount Athos. *Anal. Bioanal. Chem.* **2011**, *399*, 3065–3079. [[CrossRef](#)]
10. Liu, J.; Mouri, C.; Laursen, R.; Zhao, F.; Zhou, Y.; Li, W. Characterization of dyes in ancient textiles from Yingpan, Xinjiang. *J. Archaeol. Sci.* **2013**, *40*, 4444–4449. [[CrossRef](#)]
11. Manhita, A.; Balcaen, L.; Vanhaecke, F.; Ferreira, T.; Candeias, A.; Dias, C.B. Unveiling the colour palette of Arraiolos carpets: Material study of carpets from the 17th to 19th century period by HPLC-DAD-MS and ICP-MS. *J. Cult. Herit.* **2014**, *15*, 292–299. [[CrossRef](#)]
12. Witkos, K.; Lech, K.; Jarosz, M. Identification of degradation products of indigoids by tandem mass spectrometry. *J. Mass Spectrom.* **2015**, *50*, 1245–1251. [[CrossRef](#)] [[PubMed](#)]
13. Otlowska, O.; Slebioda, M.; Kot-Wasik, A.; Karczewski, J.; Sliwka-Kaszynska, M. Chromatographic and spectroscopic identification and recognition of natural dyes, uncommon dyestuff components, and mordants: Case study of a 16th century carpet with chintamani motifs. *Molecules* **2018**, *23*, 339. [[CrossRef](#)] [[PubMed](#)]
14. Orska-Gawryś, J.; Surowiec, I.; Kehl, J.; Rejniak, H.; Urbaniak-Walczak, K.; Trojanowicz, M. Identification of natural dyes in archeological Coptic textiles by liquid chromatography with diode array detection. *J. Chromatogr. A* **2003**, *989*, 239–248. [[CrossRef](#)]
15. Blanc, R.; Espejo, T.; López-Montes, A.; Torres, D.; Crovetto, G.; Navalón, A.; Vílchez, J.L. Sampling and identification of natural dyes in historical maps and drawings by liquid chromatography with diode-array detection. *J. Chromatogr. A* **2006**, *1122*, 105–113. [[CrossRef](#)]
16. Surowiec, I.; Quye, A.; Trojanowicz, M. Liquid chromatography determination of natural dyes in extracts from historical Scottish textiles excavated from peat bogs. *J. Chromatogr. A* **2006**, *1112*, 209–217. [[CrossRef](#)]
17. Wouters, J.; Grzywacz, C.M.; Claro, A. A comparative investigation of hydrolysis methods to analyze natural organic dyes by HPLC-PDA: Nine methods, twelve biological sources, ten dye classes, dyed yarns, pigments and paints. *Stud. Conserv* **2011**, *56*, 231–249. [[CrossRef](#)]
18. Deveoglu, O.; Torgan, E.; Karadag, R. Identification by RP-HPLC-DAD of natural dyestuffs from lake pigments prepared with a mixture of weld and dyer's oak dye plants. *J. Liq. Chromatogr. Relat. Technol.* **2012**, *35*, 331–342. [[CrossRef](#)]
19. Petroviciu, I.; Vanden Berghe, I.; Cretu, I.; Albu, F.; Medvedovici, A. Identification of natural dyes in historical textiles from Romanian collections by LC-DAD and LC-MS (single stage and tandem MS). *J. Cult. Herit.* **2012**, *13*, 89–97. [[CrossRef](#)]
20. Karpova, E.; Vasiliev, V.; Mamatyuk, V.; Polosmak, N.; Kundo, L. Xiongnu burial complex: A study of ancient textiles from the 22nd Noin-Ula barrow (Mongolia, first century AD). *J. Archaeol. Sci.* **2016**, *70*, 15–22. [[CrossRef](#)]
21. Ahmed, H.E.; Tahoun, I.F.; Elkholy, I.; Shehata, A.B.; Ziddan, Y. Identification of natural dyes in rare Coptic textile using HPLC- DAD and mass spectroscopy in museum of Faculty of Arts, Alexandria University, Egypt. *Dye. Pigment.* **2017**, *145*, 486–492. [[CrossRef](#)]
22. Tamburini, D. Investigating Asian colourants in Chinese textiles from Dunhuang (7th-10th century AD) by high performance liquid chromatography tandem mass spectrometry – Towards the creation of a mass spectra database. *Dye. Pigment.* **2019**, *163*, 454–474. [[CrossRef](#)]
23. Lech, K.; Witkos, K.; Jarosz, M. HPLC-UV-ESI MS/MS identification of the color constituents of sawwort (*Serratula tinctoria* L.). *Anal. Bioanal. Chem.* **2014**, *406*, 3703–3708. [[CrossRef](#)] [[PubMed](#)]
24. Lech, K.; Witkos, K.; Wilenska, B.; Jarosz, M. Identification of unknown colorants in pre-Columbian textiles dyed with American cochineal (*Dactylopius coccus* Costa) using high-performance liquid chromatography and tandem mass spectrometry. *Anal. Bioanal. Chem.* **2015**, *407*, 855–867. [[CrossRef](#)] [[PubMed](#)]

25. Lech, K.; Jarosz, M. Identification of Polish cochineal (*Porphyrophora polonica* L.) in historical textiles by high-performance liquid chromatography coupled with spectrophotometric and tandem mass spectrometric detection. *Anal. Bioanal. Chem.* **2016**, *408*, 3349–3358. [[CrossRef](#)]
26. Dabrowski, D.; Lech, K.; Jarosz, M. Capillary-HPLC with tandem mass spectrometry in analysis of alkaloid dyestuffs - a new approach. *Electrophoresis* **2018**, *39*, 1276–1283. [[CrossRef](#)]
27. Domon, B.; Costello, C.E. A systematic nomenclature for carbohydrate fragmentations in FAB-MS/MS spectra of glycoconjugates. *Glycoconj. J.* **1988**, *5*, 397–409. [[CrossRef](#)]
28. Cuyckens, F.; Claeys, M. Mass spectrometry in the structural analysis of flavonoids. *J. Mass Spectrom.* **2004**, *39*, 1–15. [[CrossRef](#)] [[PubMed](#)]
29. Demarque, D.P.; Crotti, A.E.; Vessecchi, R.; Lopes, J.L.; Lopes, N.P. Fragmentation reactions using electrospray ionization mass spectrometry: An important tool for the structural elucidation and characterization of synthetic and natural products. *Nat. Prod. Rep.* **2016**, *33*, 432–455. [[CrossRef](#)] [[PubMed](#)]
30. Poulin, J. A New Methodology for the characterisation of natural dyes on museum objects using gas chromatography–mass spectrometry. *Stud. Conserv.* **2018**, *63*, 36–61. [[CrossRef](#)]
31. Puchalska, M.; Orlinska, M.; Ackacha, M.A.; Polec-Pawlak, K.; Jarosz, M. Identification of anthraquinone coloring matters in natural red dyes by electrospray mass spectrometry coupled to capillary electrophoresis. *J. Mass Spectrom.* **2003**, *38*, 1252–1258. [[CrossRef](#)]
32. Lopez-Montes, A.; Blanc Garcia, R.; Espejo, T.; Huertas-Perez, J.F.; Navalon, A.; Vilchez, J.L. Simultaneous identification of natural dyes in the collection of drawings and maps from The Royal Chancellery Archives in Granada (Spain) by CE. *Electrophoresis* **2007**, *28*, 1243–1251. [[CrossRef](#)] [[PubMed](#)]
33. Witkowski, B.; Ganeczko, M.; Hryszko, H.; Stachurska, M.; Gierczak, T.; Biesaga, M. Identification of orcein and selected natural dyes in 14th and 15th century liturgical paraments with high-performance liquid chromatography coupled to the electrospray ionization tandem mass spectrometry (HPLC-ESI/MS/MS). *Microchem. J.* **2017**, *133*, 370–379. [[CrossRef](#)]
34. Calà, E.; Benzi, M.; Gosetti, F.; Zanin, A.; Gulmini, M.; Idone, A.; Serafini, I.; Ciccola, A.; Curini, R.; Whitworth, I.; et al. Towards the identification of the lichen species in historical orchil dyes by HPLC-MS/MS. *Microchem. J.* **2019**, *150*, 104140. [[CrossRef](#)]
35. Serafini, I.; Lombardi, L.; Fasolato, C.; Sergi, M.; Di Ottavio, F.; Sciubba, F.; Montesano, C.; Guiso, M.; Costanza, R.; Nucci, L.; et al. A new multi analytical approach for the identification of synthetic and natural dyes mixtures. The case of orcein-mauveine mixture in a historical dress of a Sicilian noblewoman of nineteenth century. *Nat. Prod. Res.* **2019**, *33*, 1040–1051. [[CrossRef](#)]
36. Peggie, D.A.; Kirby, J.; Poulin, J.; Genuit, W.; Romanuka, J.; Wills, D.F.; De Simone, A.; Hulme, A.N. Historical mystery solved: A multi-analytical approach to the identification of a key marker for the historical use of brazilwood (*Caesalpinia* spp.) in paintings and textiles. *Anal. Methods* **2018**, *10*, 617–623. [[CrossRef](#)]
37. Lech, K. Universal analytical method for characterization of yellow and related natural dyes in liturgical vestments from Krakow. *J. Cult. Herit.* **2020**. [[CrossRef](#)]
38. Lech, K. Dataset supporting the identification of natural dyes in yellow, orange, brown and green fibres from Krakow liturgical vestments. *Data Brief.* **2020**, *31*, 105735. [[CrossRef](#)]
39. Dąbrowski, D.; Lech, K. A Contemporary approach to study of anthraquinone dye structure by tandem mass spectrometry. In *Advances in Chemistry Research*; Taylor, J.C., Ed.; Nova Science Publishers: New York, NY, USA, 2017; Volume 34, pp. 75–106.
40. Lajko, E.; Banyai, P.; Zambo, Z.; Kursinszki, L.; Szoke, E.; Kohidai, L. Targeted tumor therapy by *Rubia tinctorum* L.: Analytical characterization of hydroxyanthraquinones and investigation of their selective cytotoxic, adhesion and migration modulator effects on melanoma cell lines (A2058 and HT168-M1). *Cancer Cell Int.* **2015**, *15*, 119. [[CrossRef](#)]
41. Szostek, B.; Orska-Gawrys, J.; Surowiec, I.; Trojanowicz, M. Investigation of natural dyes occurring in historical Coptic textiles by high-performance liquid chromatography with UV-Vis and mass spectrometric detection. *J. Chromatogr. A* **2003**, *1012*, 179–192. [[CrossRef](#)]
42. Hulme, A.N.; McNab, H.; Peggie, D.A.; Quye, A. Negative ion electrospray mass spectrometry of neoflavonoids. *Phytochemistry* **2005**, *66*, 2766–2770. [[CrossRef](#)] [[PubMed](#)]
43. Lin, L.G.; Liu, Q.Y.; Ye, Y. Naturally occurring homoisoflavonoids and their pharmacological activities. *Planta. Med.* **2014**, *80*, 1053–1066. [[CrossRef](#)]
44. Cardon, D. *Natural Dyes: Sources, Tradition, Technology and Science*; Archetype: London, UK, 2007.

45. Chen, K.; Rannulu, N.S.; Cai, Y.; Lane, P.; Liebl, A.L.; Rees, B.B.; Corre, C.; Challis, G.L.; Cole, R.B. Unusual odd-electron fragments from even-electron protonated prodiginine precursors using positive-ion electrospray tandem mass spectrometry. *J. Am. Soc. Mass Spectrom* **2008**, *19*, 1856–1866. [[CrossRef](#)]
46. Hofenk de Graaff, J.H. *The Colorful Past. Origins, Chemistry and Identification of Natural Dyestuffs*; Archetype Publications Ltd.: London, UK, 2004.

Sample Availability: Samples of the compounds are not available from the authors.



© 2020 by the authors. Licensee MDPI, Basel, Switzerland. This article is an open access article distributed under the terms and conditions of the Creative Commons Attribution (CC BY) license (<http://creativecommons.org/licenses/by/4.0/>).